AD-A085 064 NAVAL POSTGRADUATE SCHOOL MONTEREY CA F/G 21/5
A COMPARISON OF SOLID FUEL RAMJET FLOW CHARACTERISTICS AND COMB--ETC(U)
DEC 79 B A BINN

UNCLASSIFIED NL

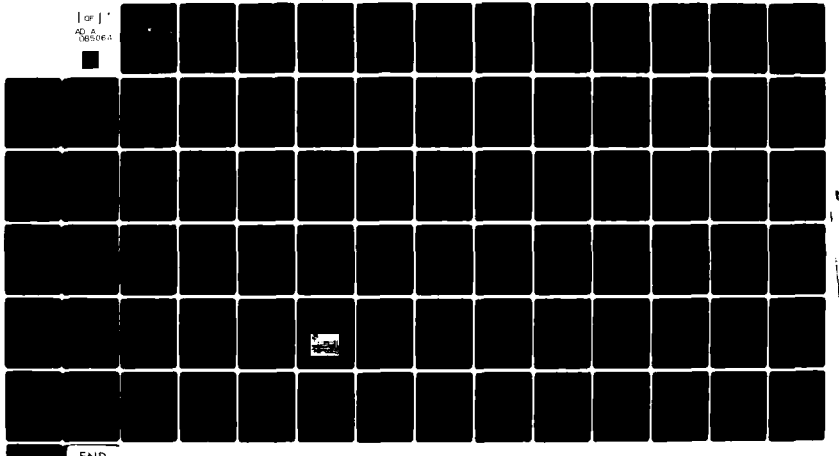

END
DATE FILMED
6-80
DTIC

NAVAL POSTGRADUATE SCHOOL

Monterey, California

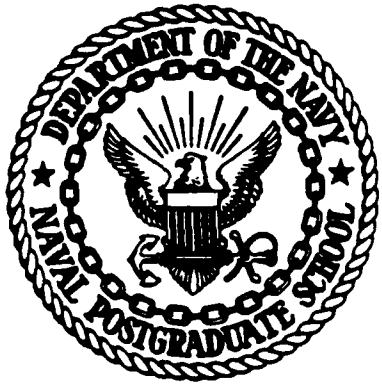

THESIS

A COMPARISON OF SOLID FUEL RAMJET FLOW CHARACTERISTICS AND COMBUSTION BEHAVIOR

by

Brian Andrew Binn

December 1979

Thesis Advisor: D. W. Netzer

Approved for public release; distribution unlimited.

UNCLASSIFIED

SECURITY CLASSIFICATION OF THIS PAGE (When Data Entered)

REPORT DOCUMENTATION PAGE	READ INSTRUCTIONS BEFORE COMPLETING FORM
1. REPORT NUMBER	2. GOVT ACCESSION NO. AD-A085064 / 3. RECIPIENT'S CATALOG NUMBER (2)
4. TITLE (and Subtitle) A Comparison of Solid Fuel Ramjet Flow Characteristics and Combustion Behavior,	5. TYPE OF REPORT & PERIOD COVERED Master's Thesis, December 1979
	6. PERFORMING ORG. REPORT NUMBER
7. AUTHOR(s) Brian Andrew Binn	8. CONTRACT OR GRANT NUMBER(s)
9. PERFORMING ORGANIZATION NAME AND ADDRESS Naval Postgraduate School Monterey, CA 93940	10. PROGRAM ELEMENT, PROJECT, TASK AREA & WORK UNIT NUMBERS N60530WR30053
11. CONTROLLING OFFICE NAME AND ADDRESS Naval Weapons Center China Lake, CA 93555	12. REPORT DATE December 1979
	13. NUMBER OF PAGES 82
14. MONITORING AGENCY NAME & ADDRESS(if different from Controlling Office) Naval Postgraduate School Monterey, CA 93940	15. SECURITY CLASS. (of this report) Unclassified
	15a. DECLASSIFICATION/DOWNGRADING SCHEDULE

16. DISTRIBUTION STATEMENT (of this Report)

Approved for public release; distribution unlimited.

17. DISTRIBUTION STATEMENT (of the abstract entered in Block 20, if different from Report)

18. SUPPLEMENTARY NOTES

19. KEY WORDS (Continue on reverse side if necessary and identify by block number)

20. ABSTRACT (Continue on reverse side if necessary and identify by block number)

An experimental investigation was conducted to determine if there is a relationship between the cold flow characteristics of velocity, pressure distribution and turbulence intensity and the reacting flow performance and combustion characteristics of a solid fuel ramjet. The effects of configuration and air flow changes on the above characteristics were examined. Average regression rates and combustion efficiencies were not significantly affected by changes in configuration. These variations in test conditions

DD FORM 1 JAN 73 1473 (Page 1) EDITION OF 1 NOV 65 IS OBSOLETE S/N 0102-014-6601

UNCLASSIFIED

SECURITY CLASSIFICATION OF THIS PAGE (When Data Entered)

significantly affected the centerline turbulence intensity but not the near-wall turbulence intensity in cold flow. The use of bypass resulted in decreases in regression rate and efficiencies for all cases. Attainable performance appears to be most strongly related to near-wall turbulence intensity/mixing and to the amount of fuel reaching the aft mixing chamber.

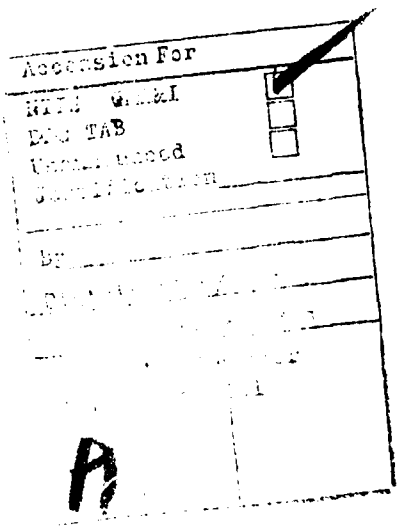

Approved for public release; distribution unlimited

A Comparison of Solid Fuel Ramjet Flow Characteristics and Combustion Behavior

by

Brian Andrew Binn
Captain, United States Air Force
B. S., United States Air Force Academy, 1972

Submitted in partial fulfillment of the requirements for the degree of

MASTER OF SCIENCE IN AERONAUTICAL ENGINEERING

from the

NAVAL POSTGRADUATE SCHOOL
December 1979

Author _____

Approved by: _____
Thesis Advisor

_____
Chairman, Department of Aeronautics

_____
Dean of Science and Engineering

ABSTRACT

An experimental investigation was conducted to determine if there is a relationship between the cold flow characteristics of velocity, pressure distribution, and turbulence intensity and the reacting flow performance and combustion characteristics of a solid fuel ramjet. The effects of configuration and air flow changes on the above characteristics were examined. Average regression rates and combustion efficiencies were not significantly affected by changes in configuration. These variations in test conditions significantly affected the centerline turbulence intensity but not the near-wall turbulence intensity in cold flow. The use of bypass resulted in decreases in regression rate and efficiencies for all cases. Attainable performance appears to be most strongly related to near-wall turbulence intensity/mixing and to the amount of fuel reaching the aft mixing chamber.

TABLE OF CONTENTS

LIST OF TABLES

Page

LIST OF FIGURES

Figure No. Page

ACKNOWLEDGMENT

I would like to take this opportunity to thank Professor David W. Netzer, Mr. Patrick J. Hickey, Mr. Ted Dunton, and my wife, Barbara. Professor Netzer's guidance and help throughout the project were invaluable in the completion of this report. Mr. Hickey's and Mr. Dunton's technical expertise aided immeasureably in the accomplishments of the experiments. And finally, the patience and understanding expressed by my family during the preparation of the report was greatly appreciated.

I. INTRODUCTION

The solid fuel ramjet (SFRJ) characteristics indicate that it may be a viable alternative to present day propulsion systems being used in intermediate range and high speed tactical weapons. The relative simplicity of the solid fuel ramjet concept, as compared to its counterparts, could lead to a highly cost effective alternative. It must first demonstrate combustion stability and efficiency over the expected operating envelope of altitudes and Mach numbers, and performance parity with today's propulsive systems.

Combustion studies on the solid fuel ramjet have been carried out at United Technologies - Chemical Systems Division since 1971 (Ref. 1). One of the findings made in the early 70's by CSD was that a sudden expansion inlet could be used to provide flame stabilization in the SFRJ as it does in liquid fuel ramjet dump combustors. The step inlet (Fig. 1) acts as a flameholder to sustain the combustion throughout the solid fuel grain. A desired characteristic of these inlets from a pressure loss standpoint is a minimum step height (h) that is capable of sustaining combustion.

The step inlet creates at least two distinct zones of combustion within the fuel grain (Fig. 1)(Ref. 2). In Zone I, also known as the recirculation zone, the flow is highly turbulent. The combustion process in this area approaches that of a well-stirred reactor. The latter process usually con-

siders the composition and all of the thermodynamic properties to be uniform throughout the volume. Downstream of flow reattachment, Zone II, a boundary layer develops and the combustion is similar to that in a hybrid rocket. A diffusion flame is located within the turbulent boundary layer between the fuel rich zone near the wall and the oxygen rich central core. The decomposition of the fuel is caused by heat being transported by convection and radiation to the solid surface.

Because of this flame geometry, some unburned fuel vapor/carbon will necessarily exit the aft end of the fuel grain. To allow for additional chemical reaction an aft mixing chamber is often employed which is larger in diameter than the fuel port. It has also been found advantageous for some fuel compositions to bypass some of the inlet air to the aft mixing chamber.

Past studies have shown that attainable performance depends on many parameters such as flameholder step size, aft mixing chamber entrance step size and length-to-diameter ratio, and bypass techniques. Variations of these parameters can change the combustion efficiency, regression rate, and flammability limits of the solid fuel ramjet.

Alternate fuels have been considered with the hope of providing higher density impulse while at the same time maintaining high combustion efficiency (Ref. 3). To date these studies have not been particularly successful and indications

are that mixing processes within the fuel grain may be more important than fuel composition (Ref. 4).

An understanding of the effects that configuration changes have on the flow and combustion characteristics is necessary to arrive at an optimum combustion efficiency. It would be very beneficial if non-reacting flow field characteristics and fundamental fuel properties could be used together to provide a priori estimation of the attainable performance.

This study was directed toward a comparison of the non-reacting flow characteristics in the solid fuel ramjet motor with the reacting flow characteristics and the obtainable performance. Later efforts will be directed toward relating fundamental fuel properties/decomposition behavior with obtainable SFRJ combustion efficiency. Data obtained from this and previous work are also necessary to validate analytical and numerical models that are being developed.

II. METHOD OF INVESTIGATION

The experimental data collected for this report was accomplished at the Solid Fuel Ramjet Facilities of the U. S. Naval Postgraduate School (Refs. 5, 6, and 7). Measurements were taken in both non-reacting and reacting tests for a variety of configurations and airflow conditions.

Non-reacting flow data consisted of static and total pressure measurements, and centerline and near-wall hot-wire anemometer studies. Nominal test conditions are listed in Table I. Static pressure was obtained with the use of wall mounted taps along the length of the ramjet motor. These values, along with total pressure measurements from a total pressure rake, were used to determine pressure distribution and velocity profiles in the ramjet motor. The hot wire anemometer data yielded quantitative and qualitative information on the turbulence intensity within the ramjet model.

To gather the desired information from the reacting flow studies, the solid fuel ramjet motor was mounted on a thrust stand. Along with the thrust data, static pressure distributions along the grain were obtained. A series of thermocouples were imbedded near the aft end of one grain in an attempt to determine the radial temperature distribution in the fuel rich region between the wall and flame. The experimental firings were conducted using Polymethylmethacrylate (PMM) fuel grains. Nominal test conditions are presented in Table II.

Fuel grains were examined after a test to determine average regression rates and, more specifically, the axial and circumferential regression patterns of the spent grains. Combustion efficiency was calculated based upon both thrust and nozzle stagnation pressure.

The information gathered in the cold flow tests were used to further characterize the flow field within the solid fuel ramjet as a function of geometric variables and bypass ratio. These cold flow data were then related to the performance and regression rate patterns obtained in the reacting flow experiments.

TABLE I

Nominal Test Conditions - Non-Reacting Flow

Run No.	Inlet Diameter (inches)	h/D	$\dot{m}_p$ ** (lbm/sec)	$\dot{m}_s$ *** (lbm/sec)	Inlet Air Temp (°F)
1	.750	.250	0.2	0.0	65
2	.750	.250	0.1	0.1	65
3	.500	.333	0.2	0.0	65
4	.500	.333	0.1	0.1	65
5	.750 w/screen	.250	0.2	0.0	65
6*	.750 w/screen	.250	0.1	0.1	65
7	.750 w/aft orifice plate	.250	0.2	0.0	65
8*	.750 w/aft orifice plate	.250	0.1	0.1	65
9	side dump/ short dome	-	0.2	0.0	65

*turbulence intensity measurements only
**primary/fuel grain air flow rate
***bypass/secondary air flow rate

TABLE II

Nominal Test Conditions - Reacting Flow

PMM Fuel Grain

Run No.	Inlet Diameter (inches)	h/D	$\dot{m}_p$ (lbm/sec)	$\dot{m}_s$ (lbm/sec)	Inlet Air Temp. (°F)
1*	.750	.250	0.2	0.0	65
2*	.750	.250	0.1	0.1	65
3	.500	.333	0.2	0.0	65
4	.500	.333	0.1	0.1	65
5**	.750 w/screen	.250	0.2	0.0	65
6**	.750 w/screen		0.1	0.1	65
7**	.750 w/aft orifice plate	.250	0.2	0.0	65
8**	.750 w/aft orifice plate	.250	0.1	0.1	65
9*	.500 w/screen	.333	0.2	0.0	65
10	.500 w/screen	.333	0.1	0.1	65
11	.500 w/aft orifice plate	.333	0.2	0.0	65
12	.500 w/aft orifice plate	.333	0.1	0.1	65
13**	side dump/ short dome	-	0.2	0.0	65
14*	side dump/ long dome	-	0.2	0.0	65

*combustion not sustained
**not attempted

III. DESCRIPTION OF APPARATUS

A. RAMJET MOTOR

The solid fuel ramjet motor was that previously used by Mady, and others, at the U. S. Naval Postgraduate School (Refs. 2, 5, 6 and 7). The motor consists of four main sections: the head-end assembly, the step insert section, the grain, and the aft mixing chamber/nozzle (Figure 2).

The head-end assembly contained the inlets for the air, the ethylene inlet for ignition, and the nitrogen purge and the cooling air inlets. Two distinct types of head-end assemblies were used during the tests. For the cold flow measurements an axial air inlet was used upstream of the step inlet as shown in Figures 2 and 4. To conduct the hot firing experiments the ramjet motor was mounted on a thrust stand. This necessitated the use of a different head-end assembly to enable the air to enter the engine from the sides. The air was then turned 90° with a wedge to enter the inlet and fuel grain (Figure 3).

The step insert section held the inlet in place. Two step inlets were used during this investigation, with inside diameters of 0.50 and 0.75 inches. These sizes resulted in h/D values of 0.333 and 0.25, respectively. The inlets were constructed such that a stainless steel 8x8 mesh (51.8% open area) screen could be attached at the grain inlet to vary the inlet distortion/turbulence intensity.

The cold flow tests and hot firings were done using the above mentioned PMM fuel grain. This fuel was selected because of its availability and wide use for basic research in hybrid rocket combustion and in studies of polymer degradation. The grains were twelve inches in length with an initial inside port diameter of 1.5 inches.

Two of the PMM grains were modified to examine the effects of a side dump/dome inlet configuration (Figure 5).

The aft mixing chamber had four bypass dumps located symmetrically around the chamber. For this study two 180° opposed dumps were used, and the remaining two were blocked off. These bypass dumps were 0.803 inches in diameter and were located 2.0 inches from the exit plane of the fuel grain. A 0.1875 inch thick orifice plate with a 1.5 inch internal diameter was located at the aft end of the fuel grain to maintain a fixed step height entering the aft chamber. Those tests which are labelled "with aft orifice plate" employed a similar orifice with a 1.0 inch internal diameter.

The aft chamber had a length to diameter ratio (L/D) of 2.93 and an inlet step h/D of .146. A pressure tap was located near the rear end of the aft chamber. A 0.5 inch diameter converging nozzle was used in the cold flow experiments to provide choked flow. A nozzle of 0.75 inch diameter was used during hot firing runs to provide a chamber pressure of approximately 60 psia.

B. AIR SUPPLY AND FLOW CONTROL SYSTEM

The main air supply was powered by a Pennsylvania air compressor that could provide air at pressures up to 150 psia. The air was fed into a reservoir and then directed to the ramjet motor. A polytherm air heater was also available if the air needed to be heated.

Standard ASME orifice flowmeters (Ref. 8) were used to measure the flow rates of the air into the motor for both primary and secondary (bypass) air. Manually operated gate valves between the orifices and the motor were used to provide the desired flow rates to the motor. Two pneumatically operated Jamesbury ball valves (operating together) either vented the primary air to the atmosphere, or allowed it to pass through the motor. The line pressures and differential pressures across the ASME orifices were recorded on a Honeywell Model 2106 Visicorder and/or a strip chart recorder.

C. INSTRUMENTATION

Flow measurements during the cold flow tests consisted of a total pressure rake, axial pressure distributions (using wall pressure taps), and centerline and side wall hot wire turbulence intensity measurements. During hot firings the axial pressure distribution was also measured as was the thrust.

1. Total Pressure Rake

A 7-probe total pressure rake was designed to axially traverse the ramjet motor from the inlet plane through the aft

mixing chamber. Figure 6 is a drawing of the rake installed in the PMM fuel grain. A mounting device was attached to the nozzle to steady the probe and allow for traversing of the motor. The probe support tube was scribed for easy determination of probe location when inside the motor. Plastic tubing connected the seven total pressure taps to a Scanivalve system, which was in turn attached to a digital D.C. voltmeter for reading of the data.

2. Static Pressure Taps

A total of 8 wall pressure taps were employed. One was located in the head-end assembly and one, as previously mentioned, in the aft mixing chamber. The remaining six were spaced in the fuel grains as shown in Figure 7. These were also connected to the Scanivalve system mentioned above. These measurements, along with the rake total pressure readings, allowed for determination of velocity profiles throughout the ramjet apparatus during non-reacting experiments. During non-reacting experiments the Scanivalve output was manually recorded. During hot firings the output was recorded on a strip chart with the Scanivalve cycled automatically.

3. Hot-Wire Anemometers

Turbulence intensity measurements were made during the cold flow experiments along the centerline of the ramjet motor and also along the side walls of the fuel grain at two circumferential positions (90^{o} and 180^{o}). The apparatus used miniature Thermo-systems Incorporated (TSI) hot wires. Figures 8

and 9 show the hot wire apparatus in the fuel grain. The hot wire was connected directly to the TSI electronic equipment. A D.C. voltmeter and a true RMS meter were used to read the hot wire output. Additionally, an oscilloscope was connected for visual observations of the hot wire output and for setting the stability prior to the measurements.

4. Temperature Profiles

To establish a radial temperature profile near the surface of the regressing fuel grain, ten chromel-alumel thermocouples were embedded approximately 1-5/8 inches from the aft end of the fuel grain. The distance of the individual thermocouples from the internal wall was graduated as shown in Figure 10. The thermocouples were connected to a Visicorder.

5. Thrust Measurement

Thrust measurement was accomplished by mounting the ramjet motor apparatus to a small thrust stand as shown in Figure 11. The head-end of the motor was mounted such that the thrust pick-up was in-line with the centerline of the engine. The transducer output was recorded on a strip chart recorder. Load cell calibration was accomplished using a pulley/weight system.

IV. EXPERIMENTAL PROCEDURES

A. CALIBRATIONS

The transducers required for the flow and thrust measuring devices were calibrated prior to the running of each test. The line pressure and differential pressure transducers and the Scanivalve were calibrated using a Heise gauge and bottled nitrogen.

B. NON-REACTING FLOW STUDIES

The desired flow rates for the test being conducted were first set by manually opening gate valves until the required differential pressures were obtained across the orifices for the amount of line pressure available. Once this was accomplished, the data could be taken. Critical to the validity of the data collected was the ability of the air compressor to supply steady air pressure to the motor. This was dependent on the demands placed on the compressor by other users. It was necessary to run the tests at times when the air supply was not being used by another facility. In initial testing, under less controlled conditions, there were fluctuations in the data that were caused by such a modulating flow from the compressor.

The nominal test conditions for the non-reacting flow studies are summarized in Table I.

1. Pressure and Velocity Distributions

The total pressure rake was axially traversed from the air inlet plane to the aft mixing chamber. All 15 wall

static and stagnation pressure readings, plus one atmospheric reading, were made when the rake was secured at each desired position. Data were taken at 1.0, 3.5, 5.0, 8.0, 12.0, 15.0, and 17.5 inches from the air inlet.

The wall static pressure distributions plotted in Figures 21 to 24 were obtained when the rake was positioned at 15.0 inches (3.0 inches into the aft mixing chamber). This position was selected to limit effects due to the blockage which occurs when the probe is within the fuel grain.

The velocity profiles could easily be determined using the static and total pressure values together with the isentropic, compressible flow relationships between the pressures, velocity, temperature, and the properties of air. The values of γ and R, which were used, were those of air on a standard day at sea level.

2. Hot-Wire Anemometer Studies

A guide was mounted as close to the hot wire as possible to steady the probe. This helped reduce the vibration of the probe considerably. Although the readings taken near the rear end of the grain and in the aft mixing chamber did not receive the benefits from the guide, the velocities in these regions were much lower and vibrations of the probe were minimal.

The centerline turbulence intensity measurements were taken at the air inlet plane, at 1 inch intervals through the first half of the grain, and then at larger intervals (depending on the test being run).

The near-wall turbulence readings were taken at a nominal radial distance of 3/32 inches from the wall. Two passes were made down the grain in order to obtain the data at 90^{o} and 180^{o} under the same flow conditions. The data were recorded at 0.5 inches from the air inlet and then at one inch intervals to 9.0 inches. It was impossible to obtain data for locations aft of 9.0 inches with the experimental set-up used in these tests. If the probe guide had been allowed to exit the aft end of the grain, the wire would have broken when it came into contact with the wall.

Using the readings from the digital D.C. voltmeter and the Ballantine true RMS meter, the turbulence intensities were determined. Although the hot wire was used in the linearized mode, many of the measurements could only be considered in a qualitative manner since intensities often exceeded 15%.

C. REACTING FLOW STUDIES

Nominal test conditions for the hot firings are listed in Table II. The procedure for setting of the required flow rates for the tests was the same as that used in the non-reacting experiments.

The motor was ignited by first setting the desired air flow rate(s), igniting a small ethylene-oxygen torch that vented in the face of the step inlet, and then bleeding in a small amount of ethylene upstream of the inlet dump. After ignition, the torch and ethylene bleed were terminated.

Combustion normally lasted for forty-five seconds. The motor was extinguished at the end of each run by simultaneously venting the air to the atmosphere and actuating the nitrogen purge system. Low pressure air was then blown through the motor for cooling.

1. Pressure Measurement

Several fuel grains were instrumented with pressure taps identical to those in the non-reacting flow studies (Figure 7). As with the cold flow tests, a fuel port pressure distribution was obtained. The aft mixing chamber pressure (combustion pressure) was also recorded on a Visicorder, in addition to the strip chart. This was necessary to obtain a continuous pressure-time trace for the duration of the firing. A highly accurate time signal was also recorded to allow determination of burn time for regression rate calculations.

2. Temperature Measurement

The air inlet temperature was recorded on a strip chart. The inlet total temperature was derived from the measure inlet static temperature and the air flow rate. This was used, along with the derived total temperature at the nozzle inlet, for computation of the combustion efficiency.

3. Regression Rate/Pattern

To determine the average regression rate ($\bar{\dot{r}}$) and the regression rate at the end of the fuel grain it was necessary to make preliminary measurements of the fuel grain prior to insertion into the ramjet motor. The grains were weighed

prior to and after each run. Based on the weight loss and the burn time of the run the average regression rate was calculated. The regression rate of the aft end was found by measuring the inside diameter of the aft end of the fuel grain prior to and after firing. It was found previously (Ref. 5) that weight loss gave a more consistent value of regression rate than the method based on aft-end diameter change.

The regression patterns, axially and circumferentially, were also of interest during this study. The regression patterns were examined by making selective cuts through the fuel grain both perpendicular and parallel to the central axis. These profiles were inspected for location of maximum regression rate and symmetry of burn pattern.

4. Thrust Measurement

The ramjet motor was mounted on a small thrust stand to measure thrust directly. The thrust transducer was connected to a strip chart recorder. A small tare was used to assure solid contact of the thrust stand against the transducer at all times. The thrust measurement was also used with other measured variables to determine combustion efficiency.

5. Calculation of Combustion Efficiencies

The efficiency of the ramjet combustion process is usually defined as a ratio of the theoretical temperature rise to that which is actually attained (Ref. 9) Because of the difficulty in measuring an average gas temperature due to the

high temperature levels, the accepted practice is to calculate the temperature of the gas based on either burner pressure or thrust.

The measurement of thrust can be suspect depending on on the experimental set-up and measuring technique. One of the main problems is the bringing of the air flow into the ramjet motor while mounted on the thrust stand. It is possible to introduce an unknown tare force which can degrade the acceptability of the measured thrust. The experimental set-up used (Fig. 11) minimized this problem by bringing the air into the head-end and aft mixing chamber through long flexible hoses from above, thereby imparting no force along the thrust line of the motor.

To determine the temperature rise efficiency the following relationship was used:

$$\eta_{\Delta T} = \frac{T_{t\ meas} - T_{t\ air}}{T_{t\ theor} - T_{t\ air}} \qquad (1)$$

$T_{t\ air}$ was determined from measurement of the temperature at the head-end of the motor. In this low velocity region, stagnation and static temperatures are virtually identical. The value of $T_{t\ meas}$ can be found using the measured pressure and mass flow rate, as previously mentioned, and the one-dimensional mass continuity relationship for flow through a choked nozzle (Ref. 10). From

$$\dot{m}_T = \frac{P_{T4}\ A^*\ g}{\sqrt{R\ T_{T4}}} \sqrt{(\gamma)\left(\frac{2}{\gamma + 1}\right)^{(\gamma+1)/(\gamma-1)}} \qquad (2)$$

the following relationship can be obtained:

$$T_{t\ meas} = \left(\frac{2\ \gamma}{R}\right)\left[\left(\frac{2}{\gamma + 1}\right)^{\frac{\gamma+1}{\gamma-1}}\right]\left[1 + \left(\frac{\gamma - 1}{2}\right) M_4^2\right]^{\frac{2\ \gamma}{\gamma-1}}\left[\frac{P_4\ A_E}{\dot{m}_T}\right]^2 \qquad (3)$$

Values of P_4, A_E, and $\dot{m}_T$ are measured quantities (station 4 is just prior to the nozzle). The NWC Pepcode computer program was used to determine the theoretical combustion temperature and required gas properties (R and γ) at the experimentally determined air-fuel ratio and inlet conditions. M_4 was determined from γ and the known nozzle contraction ratio.

The combustion efficiency based on the thrust employed the same basic formula (Eq. 1) and the value of $T_{t\ meas}$ based primarily on the thrust. From

$$F = \dot{m}_T\ u_e + (p_e - p_o)\ A_E \qquad (4)$$

the following relationship can be obtained, for a converging nozzle:

$$T_{t\ meas} = \frac{(\gamma + 1)\ g}{2\ \gamma\ R}\left[\frac{F + p_o\ A_E - \frac{P_{T4}\ A_E}{\left(\frac{\gamma+1}{2}\right)^{\gamma/\gamma-1}}}{\dot{m}_T}\right]^2 \qquad (5)$$

As can be seen there is also a dependency on P_{T4} in this equation. The required gas properties were again determined using the NWC Pepcode program.

V. RESULTS AND DISCUSSION

A. NON-REACTING FLOW EXPERIMENTS

The non-reacting flow experiments were accomplished in an attempt to characterize the flow field within the solid fuel ramjet motor for widely varying geometries and flow rates. The studies included the determination of velocity profiles, wall static pressure variation, centerline turbulence intensity, and near-wall turbulence intensity. The results obtained from these experiments will be discussed for each major geometric configuration. The results of the cold flow tests will then be examined, along with the information obtained from the reacting flow data, to determine whether the cold flow measurements can be used to predict the expected combustion efficiency and/or fuel regression pattern/rate.

1. Large Diameter Inlet, h/D = .250

This inlet (.750 in. diameter) was tested with no bypass, and with 50% of the airflow bypassed to the aft mixing chamber. The velocity profiles for these two air flow conditions are shown in Figures 13 and 14. For the case with no bypass, the flow entered the fuel grain with a high velocity (207 fps) and then as the flow expanded to the fuel port cross sectional area, decreased to 56 fps. Agreement between these values and 1-D isentropic flow values was very good. The reattachment point/region can be considered to be that point where no reverse flow occurs. This occured at approximately

4.0 inches for the case with no bypass as compared to over 8.0 inches when bypass was introduced. The reattachment point location for no bypass flow compared favorably with previous work (see Figure 12). The length of the recirculation region for the run with bypass was surprisingly long. If the flow were laminar there would be a tendency for the reattachment zone to move downstream. However, a check of the Reynolds number indicated that, as expected, the flow was very turbulent. Apparently, the flow characteristics within the aft mixing chamber affect the flame stabilization region within the fuel port. The profiles in the center portion of the aft mixing chamber were flat and essentially identical for both cases. The flow entering the aft chamber passes over a small step, similar to the inlet. The recorded velocity profiles only covered the 1 - 1/2 inches down the center of the chamber and no information on the reattachment point in the aft mixing chamber was obtained.

Figure 21 presents the axial pressure distributions in the fuel grain and one point in the aft mixing chamber. The pressure leveled off at about 5.0 inches in each case, slightly downstream of the no-bypass reattachment zone. The steady pressure for the 50% bypass situation was about 1.5% higher. This was apparently due to the slightly higher total mass flow rate. Although the mass flow through the grain was low for 50% bypass, the pressure was maintained close to that for the no-bypass situation due to the same total mass flow

through the nozzle throat. A small increase in the pressure and corresponding decrease in velocity occurred as the flow expanded into the aft mixing chamber.

Figure 25 compares the centerline turbulence intensities for the two cases. The qualitative behavior of both flows compares favorably with analytical and experimental work discussed in Reference 6. The peak intensities were located at approximately 5-1/2 and 7-1/2 inches, near the location where wall static pressures leveled off and just downstream of the reattachment regions. The turbulence intensities at the inlets were about the same indicating that the fluctuating velocity (u') was less for the bypass conditions. In the aft end of the grain, however, the fluctuating component of the velocities were nearly the same since the mean velocity ($\overline{U}$) was about half for the case of 50% bypass.

Analysis of the side and bottom wall turbulence intensities (Figures 26 and 27) indicated that, in contrast to the centerline turbulence intensities, there was no significant effect of the bypass on the position of maximum near-wall turbulence intensity in the fuel port. Bypass levels were again greater than no-bypass levels. The secondary peaks occurred at approximately 4.0 inches, near where the flow reattachment occurred with no bypass. The near-wall turbulence intensities were significantly greater than the centerline values. Comparison of side and bottom wall profiles indicated that the flow was nearly radially symmetric along the grain.

The upstream effects of the bypass on the flow seem to be significant. It moved the reattachment point downstream (as determined by the mean velocity profiles), increased the required distance for the velocity profiles to become flat, moved the peak centerline turbulence intensity downstream, and also caused an increase in the turbulence intensities for both near-wall and centerline positions. If centerline turbulence intensity could be used to characterize the regression rate pattern, the 50% bypass results could indicate that a more rapid variation in regression rate would occur along the grain. It could also be expected that the point of maximum fuel regression would take place farther downstream for the bypass case.

However, if near-wall turbulence could be used to characterize the regression pattern no significant variation would be expected between no bypass and 50% bypass.

2. Large Inlet Diameter, w/Screen, h/D = .250

This test was conducted with a wire mesh screen attached to the step inlet in order to examine the effects of inlet distortion/turbulence intensity variations. Velocity profiles, Figure 15, and pressure distributions, Figure 23, are presented for the no-bypass conditions. Bypass was not introduced with this configuration until turbulence intensity measurements were taken.

The velocity profiles were almost identical to those with no screen; showing only a slight decrease in maximum

velocity at the inlet. The screen did not seem to have any effect on the reattachment point location or the mean velocity profiles.

The pressure distribution (Figure 23) also exhibited the same characteristics as the inlet without the screen.

The effect of the screen was readily noticeable in the turbulence intensity measurements (Figures 28 to 30). The location of the peak centerline intensity was the same, but the value was much greater. Since the average velocity ($\overline{U}$) was nearly the same with or without the screen, the fluctuating velocity values (u') were much greater. As for the inlet without the screen, the peak near-wall intensities occurred farther upstream than the peak centerline intensities. The screen had little effect on the magnitude of the bottom wall intensities but decreased the side wall values.

The screen apparently introduced increased centerline turbulence without significantly affecting the mean flow characteristics or the near-wall turbulence.

3. Large Inlet Diameter, w/aft Orifice Plate, h/D = .250

In this series of experiments an orifice plate was placed at the rear of the grain. The plate had a one inch diameter hole which gave the fuel grain a 1/4 in. "lip" for the flow to pass over. This geometry should provide increased mixing of the fuel vapor and air within the fuel port.

The pressure data used to construct the velocity profiles showed large fluctuations, but the mean velocity and

pressure profiles within the fuel grain (Figures 16 and 23) were the same as without the plate. The aft-end flow restriction apparently caused large scale oscillations in the flow within the entire fuel grain. The mean location of the reattachment point appeared to be unchanged. A difference was noted in the aft mixing chamber, as expected, since the flow area was reduced by the presence of the plate. Near the grain exit and into the aft mixing chamber, the velocity increased and a large aft recirculation zone was generated.

The centerline turbulence (Figure 31) was also affected by the installation of the plate. The turbulence intensity without bypass did not peak and then drop off as it did without the plate. The values increased to a slightly higher value and remained nearly constant. The bypass condition showed a great increase in turbulence intensity within the fuel grain, indicating again that the fluctuating velocity (u') was much greater.

The near-wall turbulence intensity profiles (Figures 32 and 33) were nearly the same with and without the orifice plate, with peak intensity occurring at about 4.0 inches. It is interesting to note that the wall measurements showed the turbulence intensity to drop off after the peak value whereas the centerline values did not. The near-wall intensity values were very similar in magnitude and profile with and without the aft orifice plate. These data indicate that the effect of the plate on the higher frequency turbulence might be con-

fined to the core of the flow and to the aft mixing chamber. As noted above, very low frequency mean velocity oscillations were introduced in the flow by the aft orifice plate. Thus, increased bulk mixing occurred throughout the fuel port and increased centerline turbulence occurred in the flow at the aft end of the fuel grain where the boundary layer is thick. This behavior indicates that the orifice plate may increase fuel regression rate near the aft end and also may increase combustion efficiency. However, if near-wall turbulence dominates the regression rate behavior, very little regression rate changes would be observed.

4. Small Diameter Inlet, h/D = .333

This inlet had a diameter of 0.50 inches and was examined for the same air flow rates, with and without bypass, as the large inlet.

Figures 17 and 18 depict the velocity profiles for this case. Both conditions of air flow exhibited similar profiles with a reattachment area between 3.5 and 5.0 inches. This is the same as for the smaller step height examined earlier. Reattachment location has been shown previously to be a function of step height. It is not possible from the data presented to locate a more precise position, but the values are in general agreement with previously presented data (Ref. 6). As expected, this inlet had higher velocities at the inlet plane. Again, these compared well with 1-D isentropic flow values for the given conditions of area, air

density, and mass flow rate. The bypass condition did not cause the large scale recirculation effects on the velocity profiles within the fuel grain as it did with the .750 inch diameter inlet. The profiles in the aft mixing chamber apparently represent large scale recirculation in this region, with or without bypass. This is a marked deviation from the results of the larger inlet experiments.

The axial pressure distributions, Figure 22, show the same general characteristics as with the large inlet. The gradient from the head-end to the steady state value is noticeably greater due to the higher velocities at the inlet plane. It took slightly more distance for the pressures to level off. These results indicate that bypass has more upstream effects on the large diameter/lower velocity inlet but that the aft mixing region is more unsteady with the small diameter inlet.

Centerline and near-wall turbulence intensities are shown in Figures 34 through 36. The general characteristics of the centerline intensity profiles were in agreement with that large inlet data. The magnitudes of the centerline intensities were considerably greater, as might be expected from the higher shear rates in the forward region. Without bypass, the peak centerline intensity occurred further upstream, very near flow reattachment. The introduction of the bypass air flow increased the values of the intensity, especially in the aft portion of the grain, and the values were much higher than

with the large inlet. The highest value of intensity with bypass occurred downstream of the flow reattachment and the location where the pressure leveled off.

Near-wall turbulence intensities were less with the smaller inlet and the peak values occurred further downstream.

Higher centerline values and lower wall values, as compared to the larger step height, can be explained by the movement and location of the eddies created by the interface between the core flow and the recirculation region. The eddies formed are closer to the centerline with the small inlet and are of greater intensity initially. This could explain the occurrence of the peak centerline intensity closer to the head-end, and the greater value without bypass air. Apparently, the larger initial eddies are dissipated more rapidly as they approach the wall, since near-wall turbulence intensity was lower with the smaller inlet.

The effects of these data on the expected fuel regression rates and regression pattern depends upon whether centerline or near-wall turbulence intensity (or both) is more significant. If regression rate is a stronger function of centerline turbulence intensity the position of highest regression could be expected to occur at the aft end of the grain when bypass air is introduced. If near-wall intensity is predominant, the maximum regression rate would occur at about mid-grain. The downstream shift of peak near-wall turbulence intensity with increasing h/D is in agreement with reattachment and regression rate behavior.

5. Dump/Dome Inlet

The dump/dome inlet used in this study is shown in Figure 5 with $L_D = 0$. The airflow pattern was markedly different than for the axial step inlet. Flame stabilization is accomplished by the circulation of the flow in the dome as opposed to the flow behind the step for the axial inlet.

Figures 19 and 20 depict the velocity profiles obtained with the rake perpendicular and in-line with the dump plane, respectively. Large fluctuations in the mean velocity occurred. The profiles indicate large regions of reverse flow throughout the fuel grain caused by the swirling of the flow. The circumferential locations of the pockets of reversed flow are depicted in Figure 39. The reverse flow pocket apparently rotated around the grain. There were two symmetric corkscrew flow patterns, each emanating from one of the dumps. The flow made approximately one complete revolution from the dump plane to the grain exit.

The pressure profile (Figure 24) showed that the pressure was fairly constant throughout. With this amount of mixing, it would be expected that no large mean velocity differences would occur within the fuel grain.

The centerline turbulence intensity is depicted in Figure 37. However, the data obtained on this run might not be representative of the actual turbulence intensity in the core of the grain. Since the centerline of the grain was almost continually in a region of reverse flow, the hot wire apparatus blocked some of the flow from the hot wire.

The wall measurements were not affected by the hot wire apparatus because of the position of the wire in relation to the holder. Figure 38 depicts the near-wall turbulence intensities for a side wall position and along the bottom of the grain. As opposed to the tests with the axial inlet, there was a difference in the turbulence intensity profiles depending on the radial position. The graphs again indicate a swirling of the flow with the greatest intensities occurring when the hot wire was located in a region of reverse flow.

The velocity and turbulence intensity data indicate that the regression pattern could be very non-symmetric both circumferentially and axially. If the areas of greatest regression correspond to those regions where the near-wall turbulence intensity is greatest, a spiral regression pattern would be obtained.

B. REACTING FLOW EXPERIMENTS

A total of 12 firings were made, all with PMM fuel grains. (Results from the eight successful reacting flow experiments are shown in Table III.)

Regression rates, fuel flow rates, and air fuel ratios were calculated based upon both weight change and diameter change. Weight loss calculation values were used for inputs to Pepcode and for calculation of combustion efficiencies.

Ignition time for the tests varied. A nominal value between 3 and 4 seconds was desired. The time listed in Table III

represents the total time the ignition switch was held (switch time). In some tests multiple ignition attempts were required before ignition was obtained (shown by the large ignition times). There was also a slight delay between the time the ignition switch was depressed and when the igniter lit. Extreme ignition times affect the calculated data somewhat by altering the regression rates and therefore the other calculated values. For further refinement, an ignition test could be made to determine the average weight loss per second of ignition. The ignition weight loss could then be subtracted from the initial grain weight, prior to calculation of desired parameters.

Calculated values of regression rate and temperature rise efficiency based on pressure were in general agreement with the previous work accomplished by Mady and Netzer (Ref. 6). The regression rates obtained by Boaz (Ref. 5) under similar conditions also were in accord. Combustion efficiencies were not calculated by Boaz. Differences in both regression rate and efficiencies with the data of Hewett (Ref. 7) were noted. It was reported that the differences between the results of Hewett and Mady (and therefore the present results) might possibly have been caused by variations in manufacturing methods during the curing process of the PMM fuel.

The combustion efficiencies based on pressure for repeated runs were in close agreement. Although most parameters for the repeated runs were close, large run to run variations

in the efficiency based on thrust occurred. Combustion efficiency determined from pressures varies directly as the square of total pressure over mass flow. The efficiency found from thrust varies as the square of (thrust - pressure) over mass flow. Possible causes for the variations could be inaccuracy in the measurements or the sensitivity of the calculation to errors in measurement. The small differences in thrust and pressure between runs is magnified by the fact that the equation takes the difference between the two values.

An initial run made with the pressure taps in the fuel grain yielded a pressure distribution qualitatively similar to that attained in cold flow. However, the regression pattern of the fuel grain was altered in the vicinity of the pressure taps. This apparently resulted from local disturbances introduced within the boundary layer by the pressure taps. The regression rate in the immediate vicinity of the taps was higher than that at other areas of the grain. A concave circular area was present with one side flared in the direction of the flow. Those taps located in the recirculation region had the flared end pointing toward the head-end, while those aft of the reattachment point flared downstream. This was further evidence of the reverse flow direction in the recirculation zone. A possible application of this behavior could be the controlling of regression rate at desired areas by selectively boring holes into the core.

Since pressure distributions were not of primary importo this study, it was decided to accomplish the remainder of the runs with fuel grains without pressure taps. This allowed comparison with previous work and did not introduce unknown factors into the computation of regression rates and combustion efficiencies.

1. Large Diameter Inlet, h/D = .250

Attempts to ignite and sustain combustion with the .750 inch diameter step inlet were unsuccessful. The small step height (h) did not provide a large enough recirculation region to maintain the flame. Results by Boaz and Netzer (Ref. 5) also showed this to be the case.

To obtain information on the effects of the inlet screen and aft orifice plate it was decided to conduct these hot firings using the small diameter inlet (h/D = .333). Although cold flow data were not available for this specific configuration, data were available for the large inlet with the screen and aft orifice plate. The results can be compared if it is assumed that the same general changes in the characteristics of cold flow result with either inlet.

2. Small Diameter Inlet, h/D = .333

Four firings were made with this configuration; two with no bypass and two with 50% of the total air flow bypassed to the aft mixing chamber. The data from runs with similar air flow conditions were in very close agreement, except for the efficiencies based on thrust (probably for reasons noted earlier).

As expected with this type of axial inlet, the regression pattern was circumferentially symmetric at all points along the grain. This was true for all firings accomplished. The axial regression patterns varied between the two different cases. The non-bypass point of maximum regression was located at approximately 4.5 inches from the head-end. From the cold flow data, this corresponded to the peak in centerline turbulence intensity (Fig. 34). Side and bottom wall turbulence intensities (Figs. 35 and 36) peaked only slightly farther downstream. Since the maximum regression point was not a sharply defined position, it was impossible to distinguish from these runs if there was a better correspondence of maximum regression rate position with centerline or near-wall turbulence intensity. Both cold flow intensities increased to a maximum and then decreased as did regression rate.

The firings with bypass moved the point of maximum regression rate slightly downstream and the regression rate did not decrease from the maximum point to the aft end compared to that for the non-bypass conditions. The cold flow centerline turbulence continued to rapidly climb in the aft portion of the grain. If centerline turbulence affects the wall regression rate, the latter would be expected to continue to increase with axial distance. Bypass did cause the near-wall turbulence to level-off toward the aft end of the fuel grain (data were taken only to the 9 inch position). Near-wall turbulence intensities were also slightly higher for

the case with bypass. These results indicate that near-wall turbulence intensity better correlated with regression behavior than did centerline turbulence intensity. This might be expected since the fuel layer is quite thin and the flame is normally located very near the wall.

3. Small Diameter Inlet, w/Screen, h/D = .333

The test with no bypass air flow would not sustain combustion. Combustion was attained for the case of 50% bypass. For cold flow, the screen was observed to significantly increase the centerline turbulence intensity. This amount of turbulence apparently greatly affected the mass transport of air into the recirculation region. This could possibly cause the normally fuel rich recirculation zone to be saturated with air, thereby quenching the combustion reaction. The reduction of the air inlet velocity (mean and fluctuating component) with the use of bypass was apparently enough to allow the flameholder to sustain combustion in the grain.

The inlet screen had no noticeable effect on the average regression rate of the fuel grain or any other calculated parameters. What was observable was a large difference in the location of the point of maximum regression. This was located at 2.0 inches (vs. approximately 4.5 inches with no screen) from the head-end and was more sharply defined than the case without the screen. Besides the head-end effect, there was also an increase (although slight) in the regression rate near the aft end of the grain.

The significant forward movement of the maximum regression point was not anticipated based upon the behavior of either cold flow near-wall or centerline turbulence intensity. The reason for the increase of the regression near the aft end is also not clear. Figure 29 shows a trend toward increasing turbulence intensity in this region, but this was also the case with no inlet screen. This behavior may be primarily due to the effects of the bypass flow on the near-wall turbulence rather than the inlet screen.

4. Small Diameter Inlet, w/Aft Orifice Plate, h/D = .333

The inclusion of the smaller diameter aft orifice plate (1.0 vs. 1.5 inches) did not appreciably change the performance of the ramjet motor in either the non-bypass or bypass flow conditions as compared to the motor with the larger diameter orifice plate. The data may indicate a slight increase in average regression rate and combustion efficiency. The plate did not affect the location of maximum regression. In all cases it was located at approximately 5.0 inches. This corresponds primarily to the location of the near-wall turbulence intensity peak in cold flow. As with the case with the smaller diameter orifice plate, the 50% bypass condition caused a more uniform regression pattern throughout the grain.

Combustion pressure/thrust oscillations were noticed for all runs using 50% bypass. They were not observed for the non-bypass condition. The frequency and/or amplitude could not be determined precisely because of the recording

speed and the line length connecting the motor to the pressure transducer. Results by Mady (Ref. 6) showed it to be about 150 Hz. and approximately 20% of chamber pressure. The magnitude of the oscillations observed in the present tests were approximately 10% of the chamber pressure. This behavior may be linked to the interaction of the core flow and the bypass air in the aft mixing chamber. The smaller aft orifice plate also caused an additional characteristic. Combustion oscillations occurred periodically (approximately every 6 seconds) for short periods of time. This showed up as small peaks in pressure/thrust time traces. This behavior apparently resulted from the higher velocity of the core flow entering the aft mixing chamber together with the smaller orifice diameter. The size of the aft orifice plate hole might be critical in avoiding certain undesirable oscillations in the flow and performance.

5. Dump/Dome Inlet

Attempts to sustain combustion with the Dump/Long Dome inlet were unsuccessful. The ethylene was bled into the air flow in one of the inlets and the igniter was positioned slightly downstream of the dumps. Ignition did occur, but the combustion could not be sustained once the igniter was turned off. The initial attempt had all the airflow entering the head-end. To test the possibility that the inlet velocity/turbulence was too high, a test was tried with 50% of the

air bypassed to the aft mixing chamber. This decrease in inlet velocity did not have any effect on the ability of this configuration to sustain combustion.

Cold flow tests showed extremely high turbulence intensities in the inlet/dome region. It is quite possible that the intensity was too great (velocities too high) for the flame to stabilize in the dome area. Future experiments should be conducted in which the dump ports are enlarged to decrease the velocity. In addition, one large dump rather than two 180° opposed inlets should be examined both in cold and reacting flows. No attempts were made to fire the Dump/Short Dome inlet.

6. Thermocouple Temperature Distribution

The experiment to establish a qualitative radial temperature profile near the surface of a regressing fuel grain was not a total success. As the fuel grain burned, the section of the grain where the thermocouples were mounted burned out rapidly, leaving a radial hole in the grain. The test was terminated after a very short burn time. The Visicorder recording did show a sequential pattern of exposure of the first few thermocouples before failure. The information obtained did show that it will be possible to gather information from this type of test if a better method of securing the thermocouples is found.

VI. CONCLUSIONS AND RECOMMENDATIONS

The changes incorporated in the solid fuel ramjet motor, which included the attachment of a screen to the inlet and an aft orifice plate, did not have an appreciable effect on the calculated performance parameters. Primary effects of these devices were on the magnitude and profile of centerline turbulence intensity. Near-wall turbulence values were not greatly affected. This result and the observed effect of pressure taps on the fuel regression rate indicate that near-wall turbulence may be the cold flow parameter that can be used most successfully to predict fuel regression patterns in reacting flows.

These results also suggest that large scale change in the core flow characteristics are not going to increase the performance of the motor. Major increases in the efficiency can probably be obtained only by either increased reaction rates taking place in the aft mixing chamber, or by significantly increasing the mixing in the region of the diffusion flame within the fuel port. Of course, the configuration of the aft mixing chamber will play an important part in determining the optimum increase in efficiency. Future studies should examine the flow field effects obtained by changing the aft mixing chamber h/D and length to diameter ratio.

As discussed above, the one test with the pressure taps suggested that the regression rate is closely linked with

near-wall disturbances. The near-wall turbulence intensities did not vary appreciably between the different configurations. The latter measurements were made along the walls of the motor that were not instrumented with the pressure taps. Additional tests should be made measuring the turbulence intensity along the wall with the pressure taps, with particular attention to the area near the taps.

Additional testing needs to be accomplished to resolve anomalies between combustion efficiencies based on thrust. Also, changes to the inlet of the Dump/Dome configuration should allow for ignition and combustion so that corresponding regression characteristics can be examined. The inclusion of fundamental fuel properties in future work should allow for a good method of estimation of the attainable performance and burning characteristics based on the cold flow data for a proposed configuration.

REFERENCES

1. Naval Weapons Center Technical Publication 5378, Performance Evaluation of Experimental Solid Ramjet Fuels, by United Technology Center, November 1972.

2. Naval Postgraduate School Report 57NT74081, Flow Characteristics in Solid Fuel Ramjets, by J. T. Phaneuf, Jr. and D. W. Netzer, July 1974.

3. Burdette, W. and Reed, R. Jr., Navy High Energy Solid Ramjet Fuel Program, paper presented at 1979 JANNAF Propulsion Symposium, Anaheim, California, 5-9 March 1979.

4. Schadow, K. C., Solid Fuel Ramjet Evaluation, paper presented at 16th JANNAF Combustion Meeting, Monterey, California, 10-14 September 1979.

5. Naval Postgraduate School Report 57NT73031A, An Investigation of the Internal Ballistics of Solid Fuel Ramjets, by L. D. Boaz and D. W. Netzer, March 1973.

6. Naval Postgraduate School Report 67NT77092, An Investigation of the Combustion Behavior of Solid Fuel Ramjets, by C. J. Mady, P. H. Hickey, and D. W. Netzer, September 1977.

7. Naval Postgraduate School Report 67-78-008, Application of Light Extinction Measurements to the Study of Combustion in Solid Fuel Ramjets, by M. E. Hewett and D. W. Netzer, November 1978.

8. Flow Measurement - Supplement to Power Test Codes, v.19.5;4, The American Society of Mechanical Engineers, 1959.

9. Chemical Propulsion Information Agency Publication 276, Recommended Ramburner Test Reporting Standards, by J. B. McVey and others, March 1976.

10. Shapiro, A. H., The Dynamics and Thermodynamics of Compressible Fluid Flow, v.1, pp. 85-154, Ronald Press, 1953.

TABLE III

Results From Reacting Flow Experiments

Inlet Type	h/D = .333							
F Condition	100/0	100/0	50/50	50/50	Aft Orifice Plate 100/0	Aft Orifice Plate 100/0	Aft Orifice Plate 50/50	Inlet Screen 50/50
$\dot{m}_p$ (lbm/sec)	.204	.197	.112	.112	.201	.198	.109	.109
$\dot{m}_s$ (lbm/sec)	0.0	0.0	.106	.108	0.0	0.0	.105	.106
$\dot{m}_t$ (lbm/sec)	.223	.215	.230	.234	.219	.217	.229	.227
t_{ign} (sec)	3.26	24.0	3.26	7.5	3.0	4.5	10.4	3.0
t_{burn} (sec)	47.2	41.5	48.3	46.9	50.4	46.8	46.7	46.6
$\dot{r}_{wt}$ (in/sec)	.00639	.00658	.00462	.00493	.00656	.00687	.00543	.00463
A/F	11.34	10.83	17.58	16.56	10.79	10.25	14.4	17.6
A/F_{port}	----	----	9.01	8.29	----	----	7.32	8.92
p_4 (psia)	53.8	52.7	46.8	48.7	54.1	55.2	50.0	47.2
F(lbf)	23.8	22.5	19.0	18.5	22.5	23.8	19.5	17.6
$T_{T4\ press}$ ($^{\circ}$R)	3082	3153	2182	2295	3171	3376	2516	2285
$T_{T4\ thrust}$ ($^{\circ}$R)	3243	3078	2038	1720	2827	3274	1985	1690
$T_{T4\ theor}$ ($^{\circ}$R)	3522	3621	2662	2763	3632	3750	3026	2655
$\eta_{\Delta T\ press}$	85.4	84.9	77.6	79.2	85.2	88.4	79.7	82.7
$\eta_{\Delta T\ thrust}$	90.7	82.5	70.8	53.6	74.2	85.3	58.5	54.8

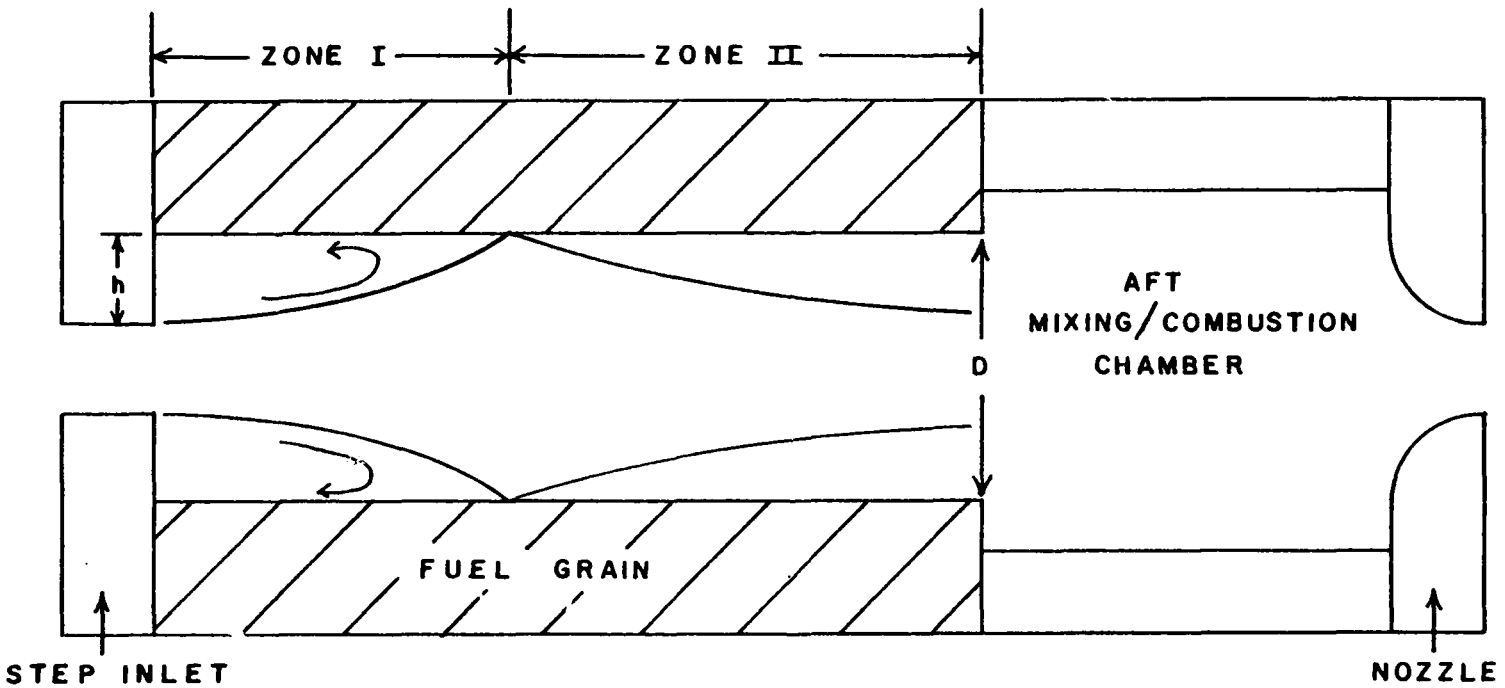

Fig. 1. Schematic of Solid Fuel Ramjet Combustion Process

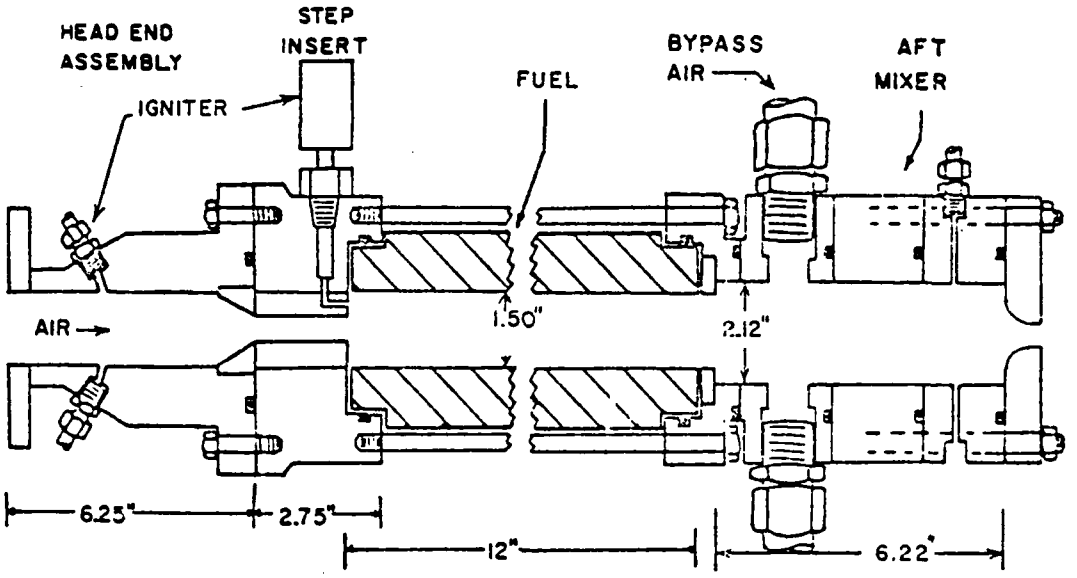

Fig. 2. Schematic of Solid Fuel Ramjet
(Fig. 1 from Ref. 7)

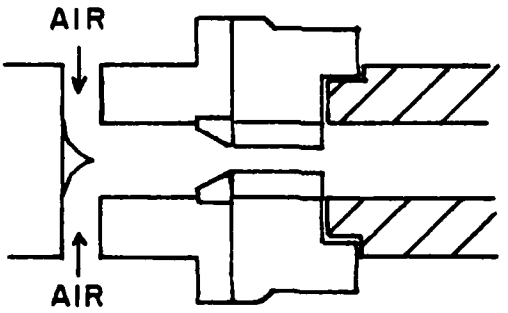

Fig. 3. Schematic of Air Inlet System for Engine on Thrust Stand

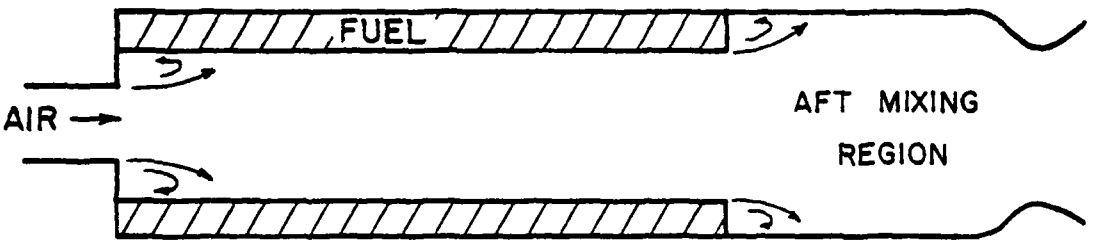

Fig. 4. Solid Fuel Ramjet Flow, Axial Inlet

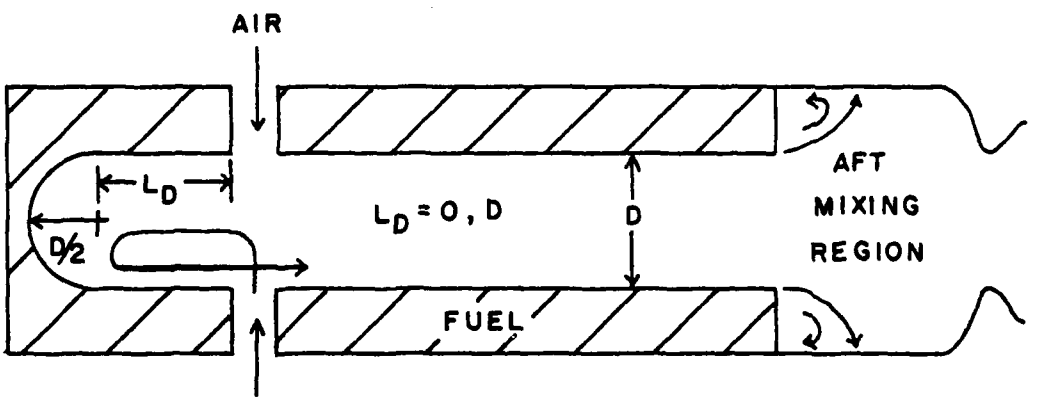

Fig. 5. Solid Fuel Ramjet Flow, Dump/Dome Inlet

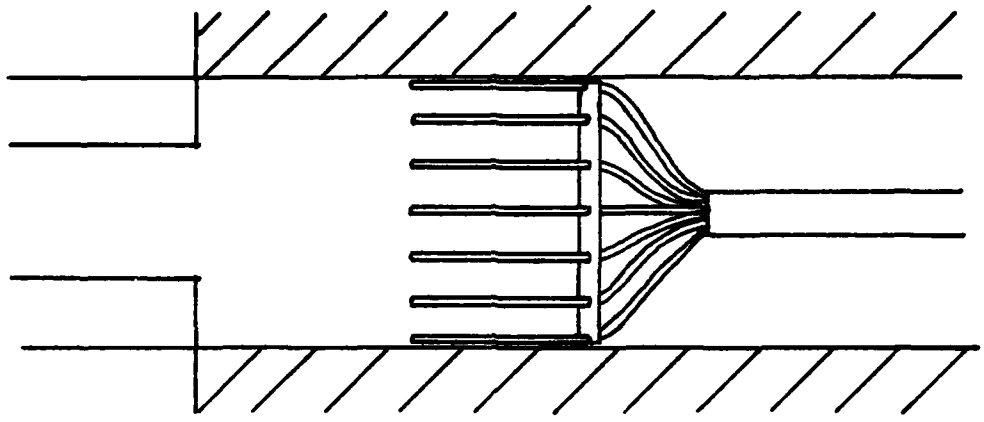

Fig. 6. Total Pressure Probe in Fuel Grain

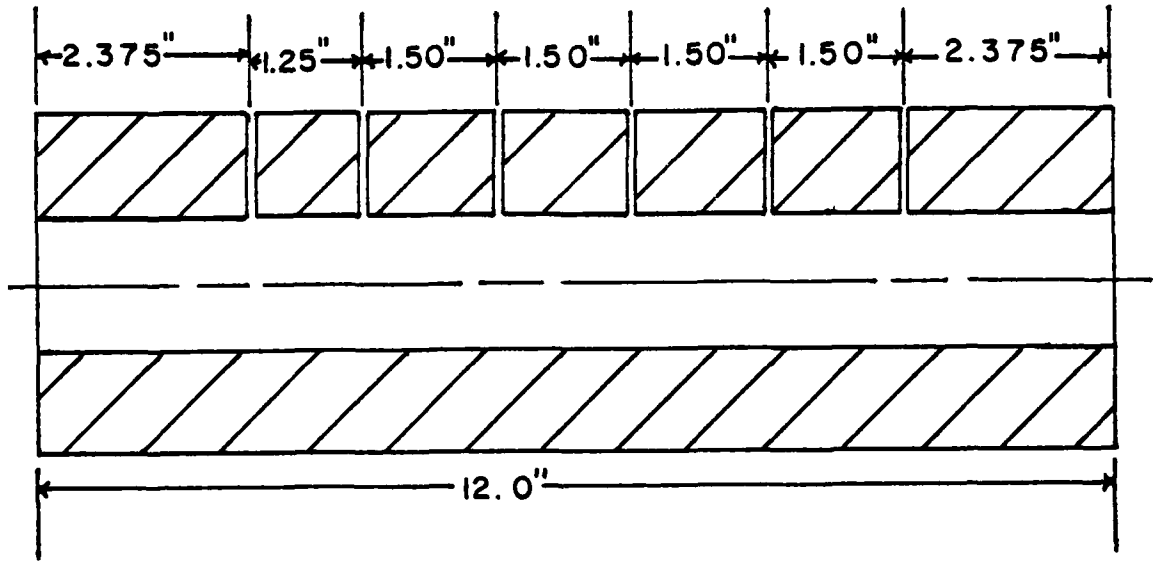

Fig. 7. Pressure Tap Locations in PMM Fuel Grain

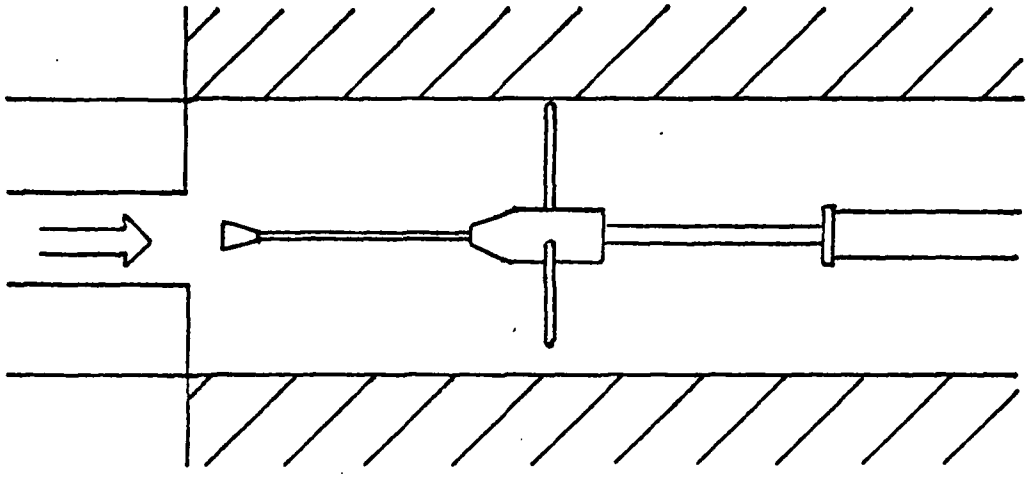

Fig. 8. Centerline Hot Wire Probe

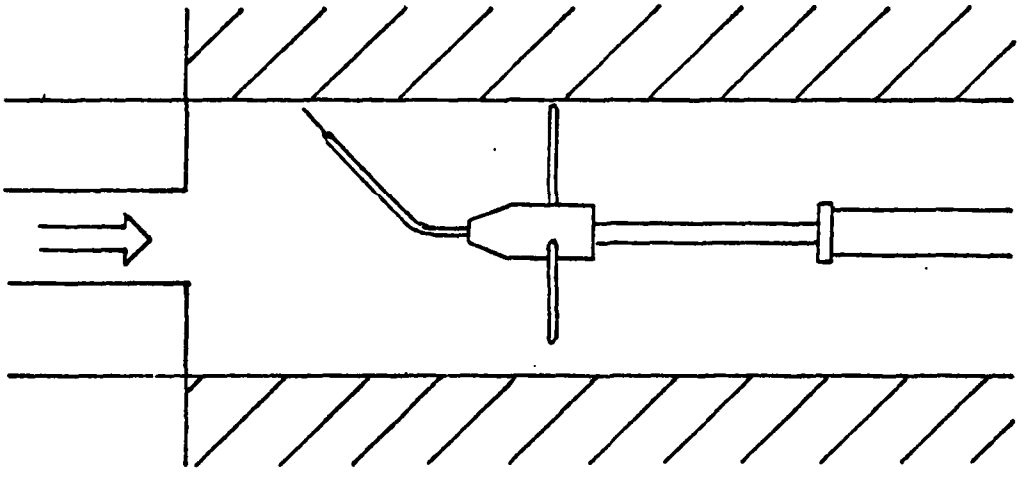

Fig. 9. Near-Wall Hot Wire Probe

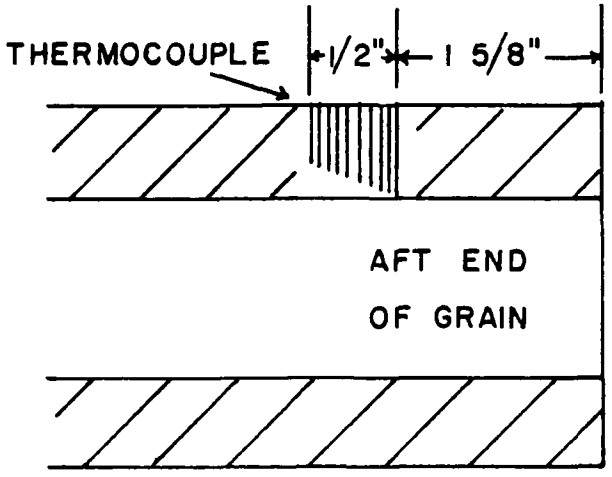

Fig. 10. Thermocouple Locations in Fuel Grain

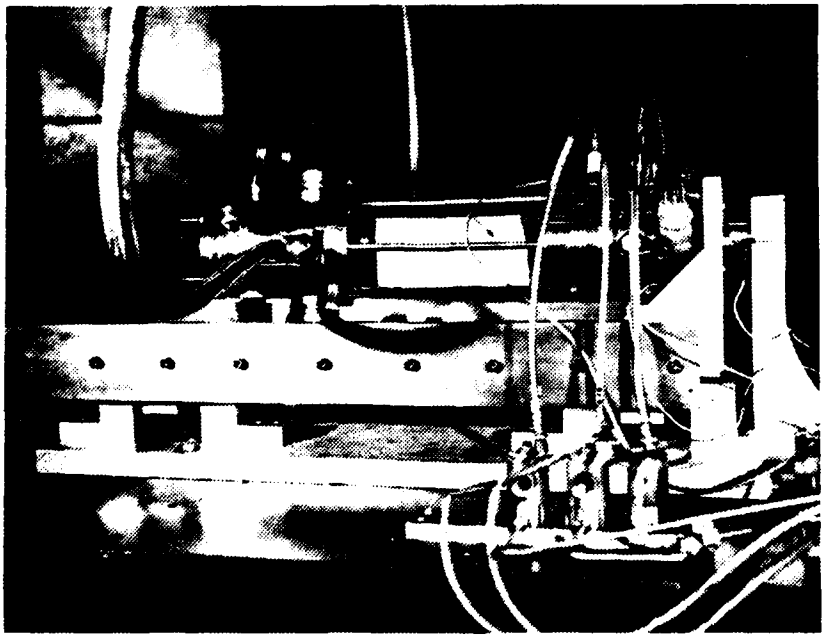

Fig. 11. Solid Fuel Ramjet on Thrust Stand

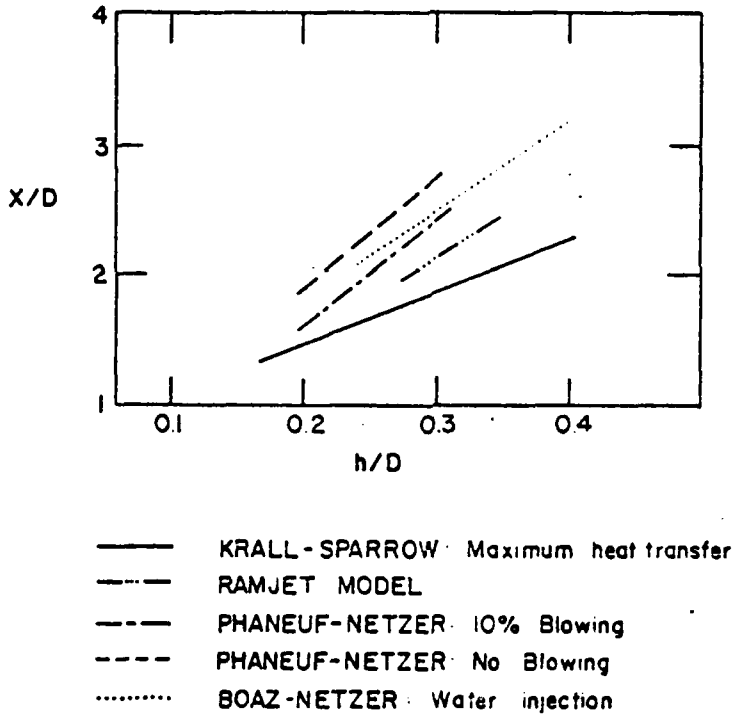

Fig. 12. Reattachment Locations for Axisymmetric Flows (Fig. 7 from Ref. 6)

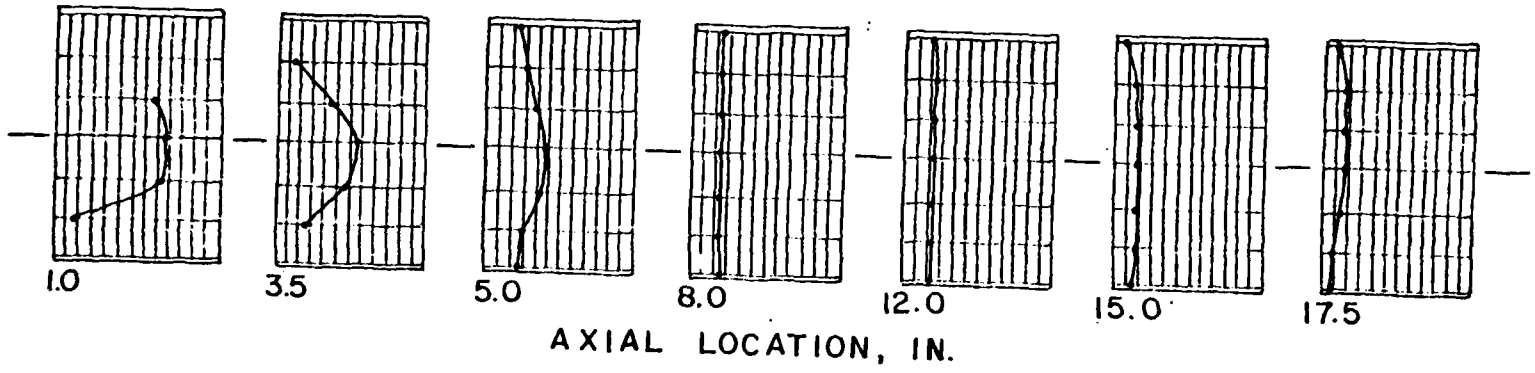

Fig. 13. Velocity Profiles, h/D = .250, P_{nom} = 55.9 psia, $\dot{m}_p$ = .198 lbm/sec

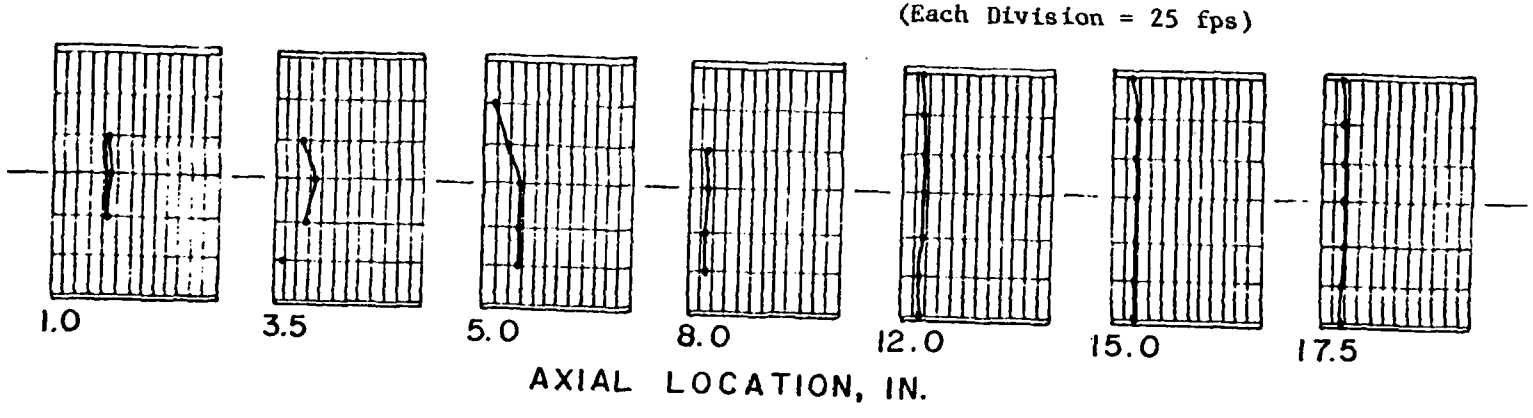

Fig. 14. Velocity Profiles, h/D = .250, P_{nom} = 56.5 psia, $\dot{m}_p$ = .104 lbm/sec, $\dot{m}_s$ = .102 lbm/sec

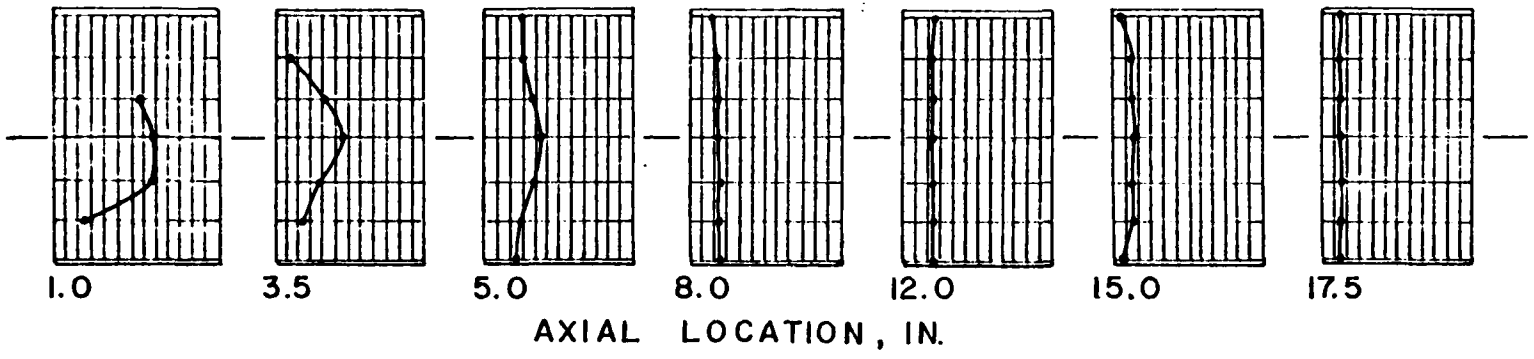

Fig. 15. Velocity Profiles, h/D = .250 w/Screen, P_{nom} = 58.2 psia, $\dot{m}_p$ = .205 lbm/sec

(Each Division = 25 fps)

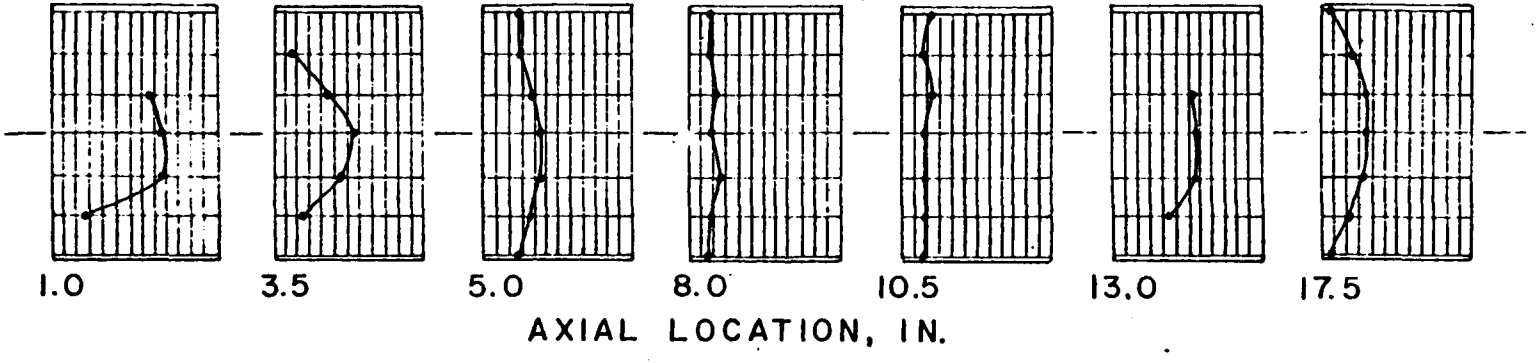

Fig. 16. Velocity Profiles, h/D = .250 w/Aft Orifice Plate, P_{nom} = 59.4 psia, $\dot{m}_p$ = .205 lbm/sec

(1 Division = 50 fps for 1 in. Profile)

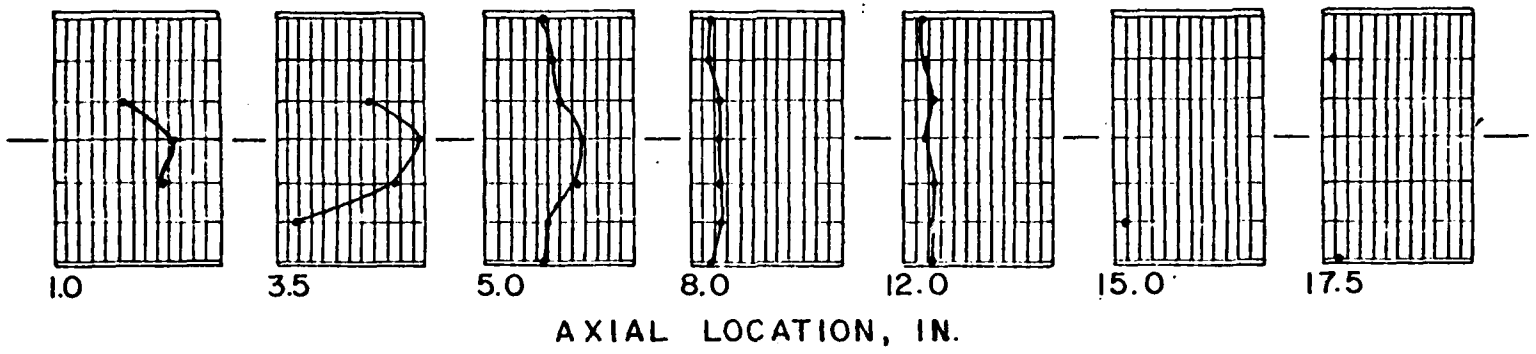

Fig. 17. Velocity Profiles, h/D = .333, P_{nom} = 59.7 psia, $\dot{m}_p$ = .207 lbm/sec

(Each Division = 25 fps)

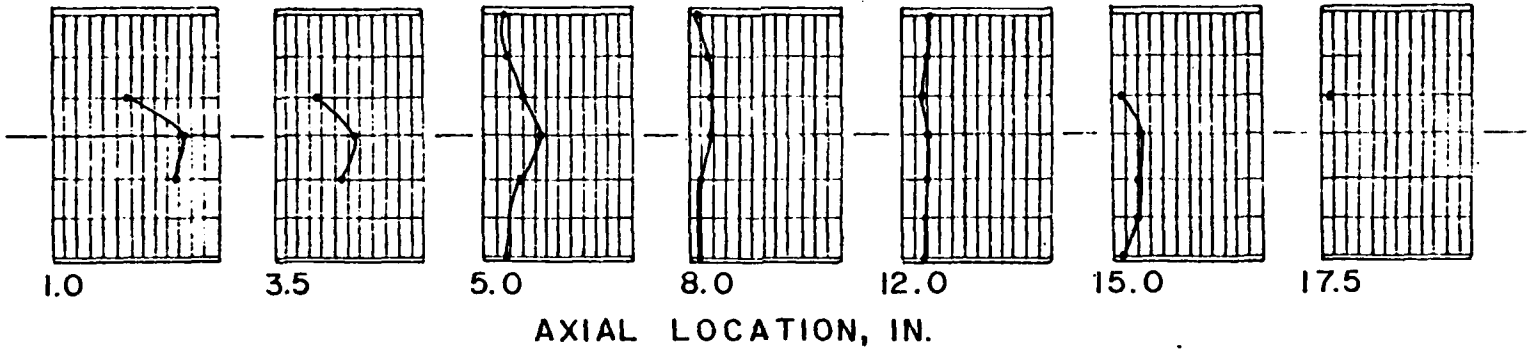

Fig. 18. Velocity Profiles, h/D = .333, P_{nom} = 60.3 psia, $\dot{m}_p$ = .107 lbm/sec, $\dot{m}_s$ = .105 lbm/sec

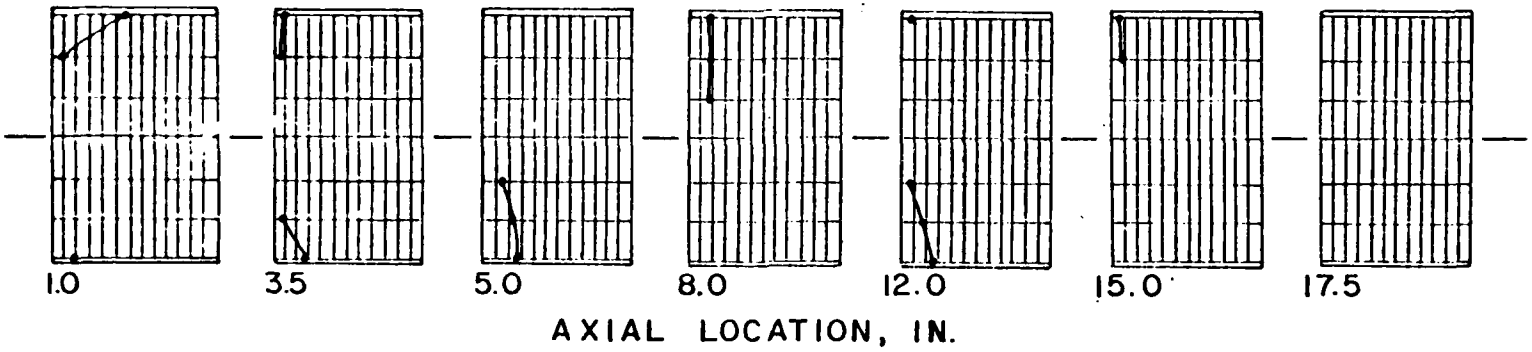

Fig. 19. Velocity Profiles, Dump/Dome Inlet, P_{nom} = 55.5 psia, $\dot{m}_p$ = .201 lbm/sec, (perpendicular to dump plane)

(Each Division = 25 fps)

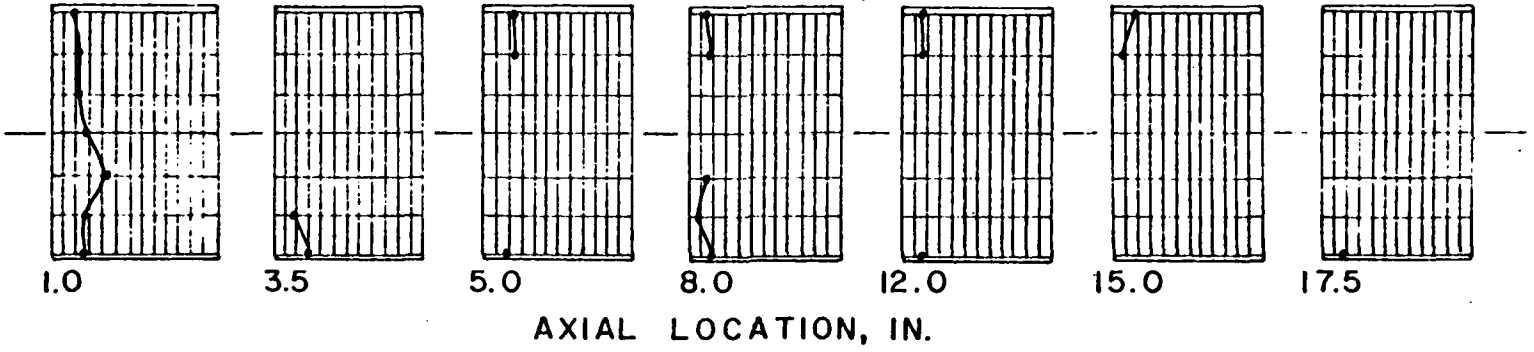

Fig. 20. Velocity Profiles, Dump/Dome Inlet, P_{nom} = 55.5 psia, $\dot{m}_p$ = .201 lbm/sec, (in-line with dump plane)

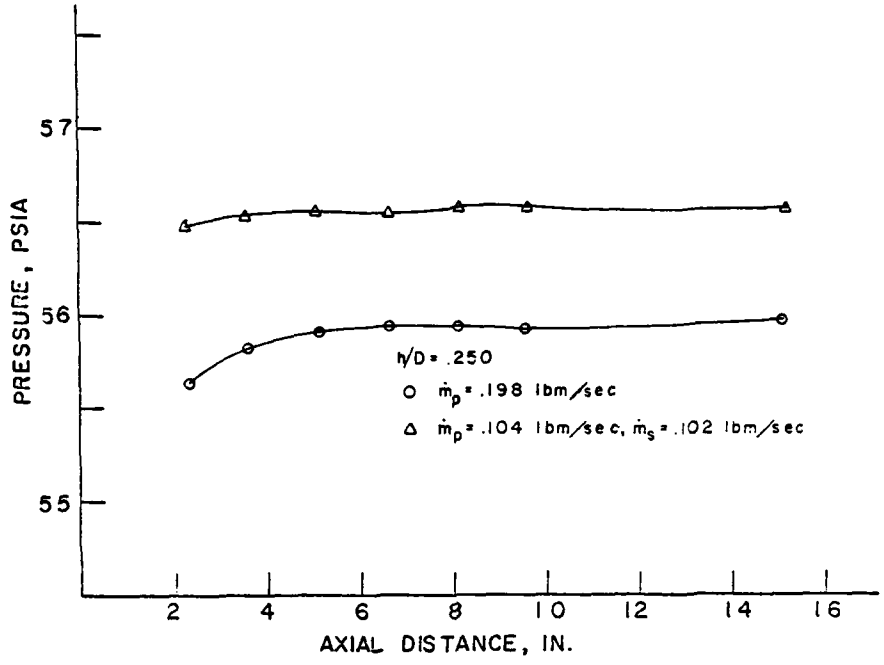

Fig. 21. Axial Pressure Distributions, h/D = 0.250

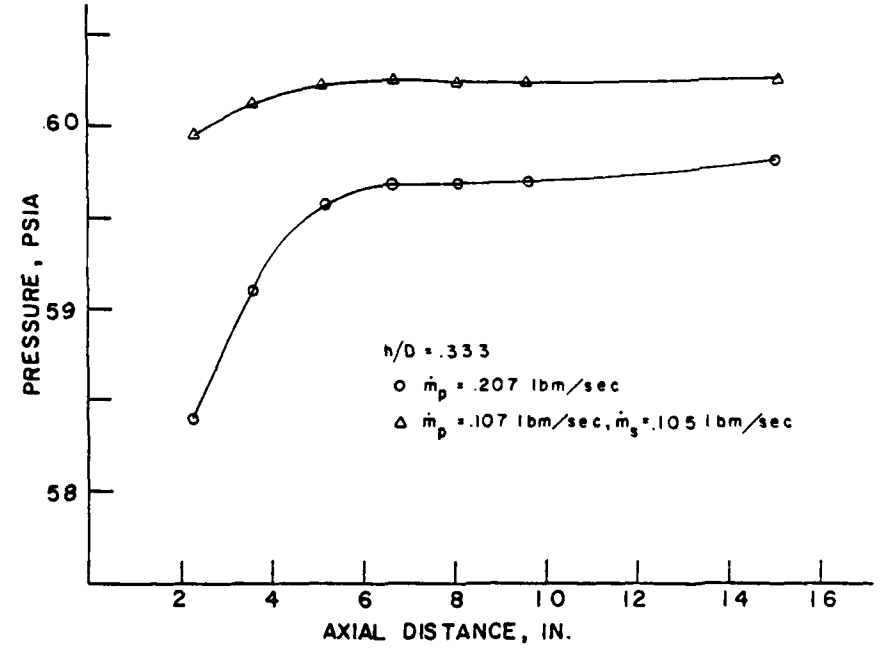

Fig. 22. Axial Pressure Distributions, h/D = 0.333

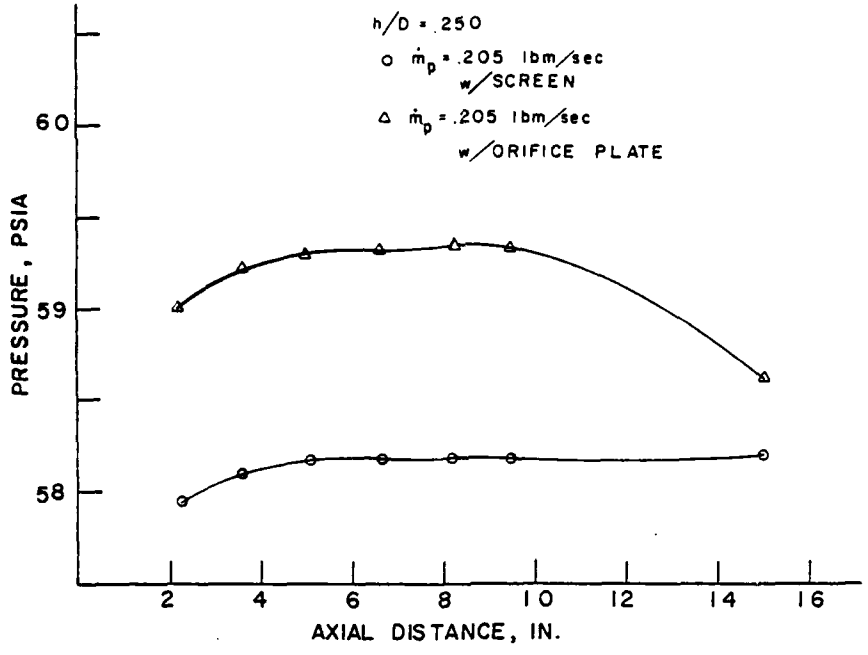

Fig. 23. Axial Pressure Distributions, Screen and Aft Orifice Plate

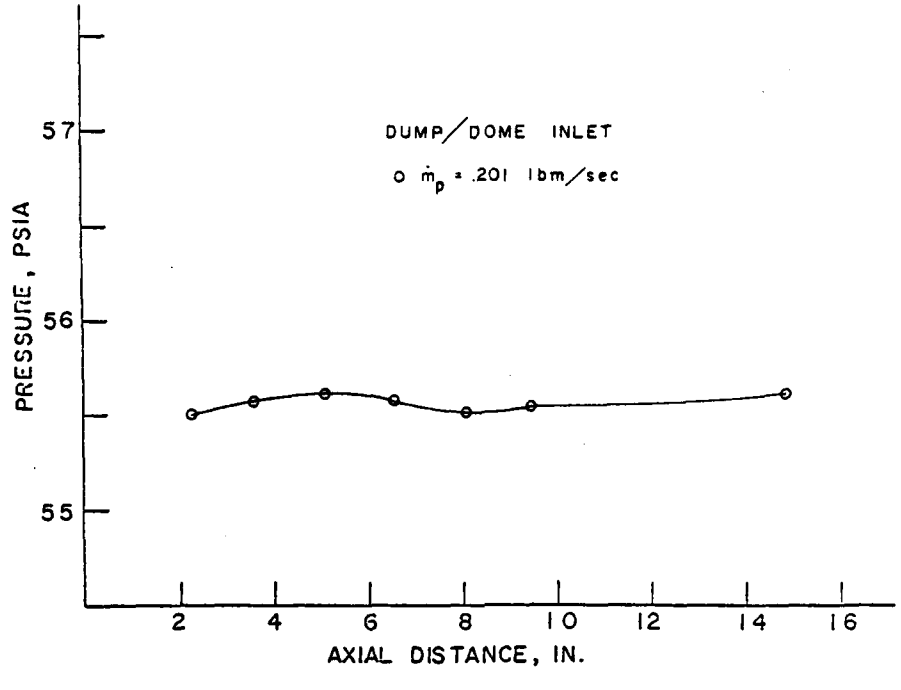

Fig. 24. Axial Pressure Distributions, Dump/Dome Inlet

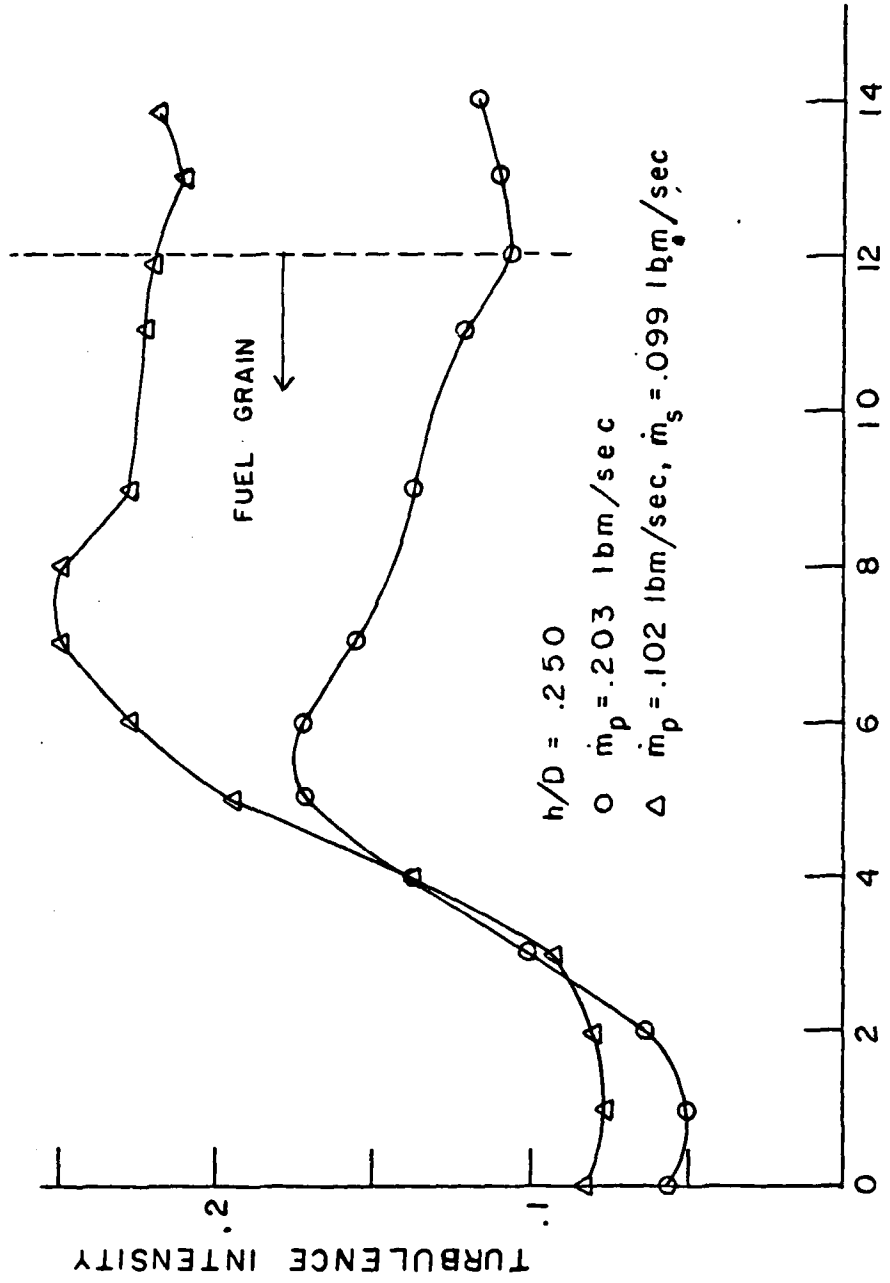

Fig. 25. Centerline Turbulence Intensity, h/D = 0.250

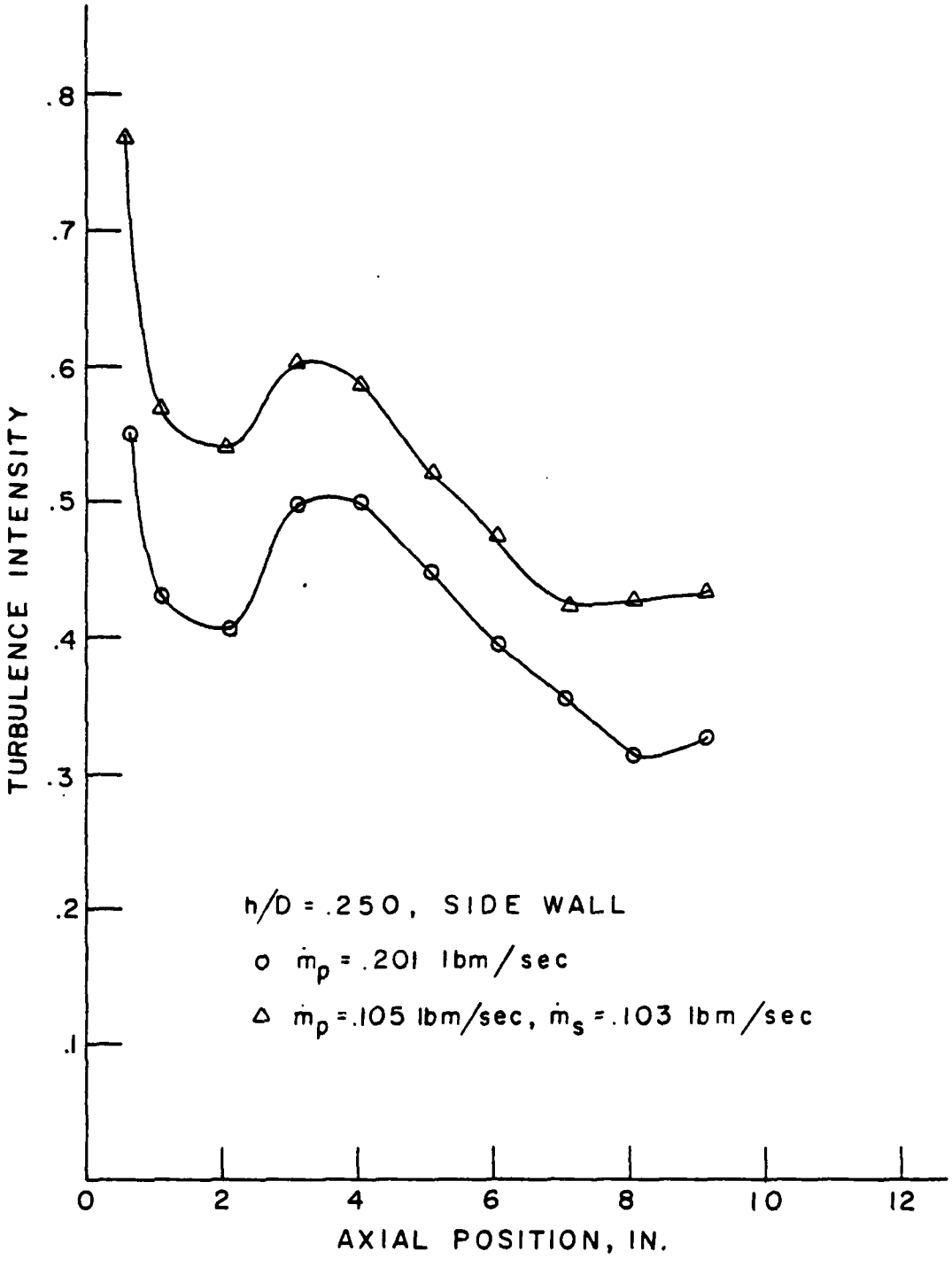

Fig. 26. Side Wall Turbulence Intensity, h/D = 0.250

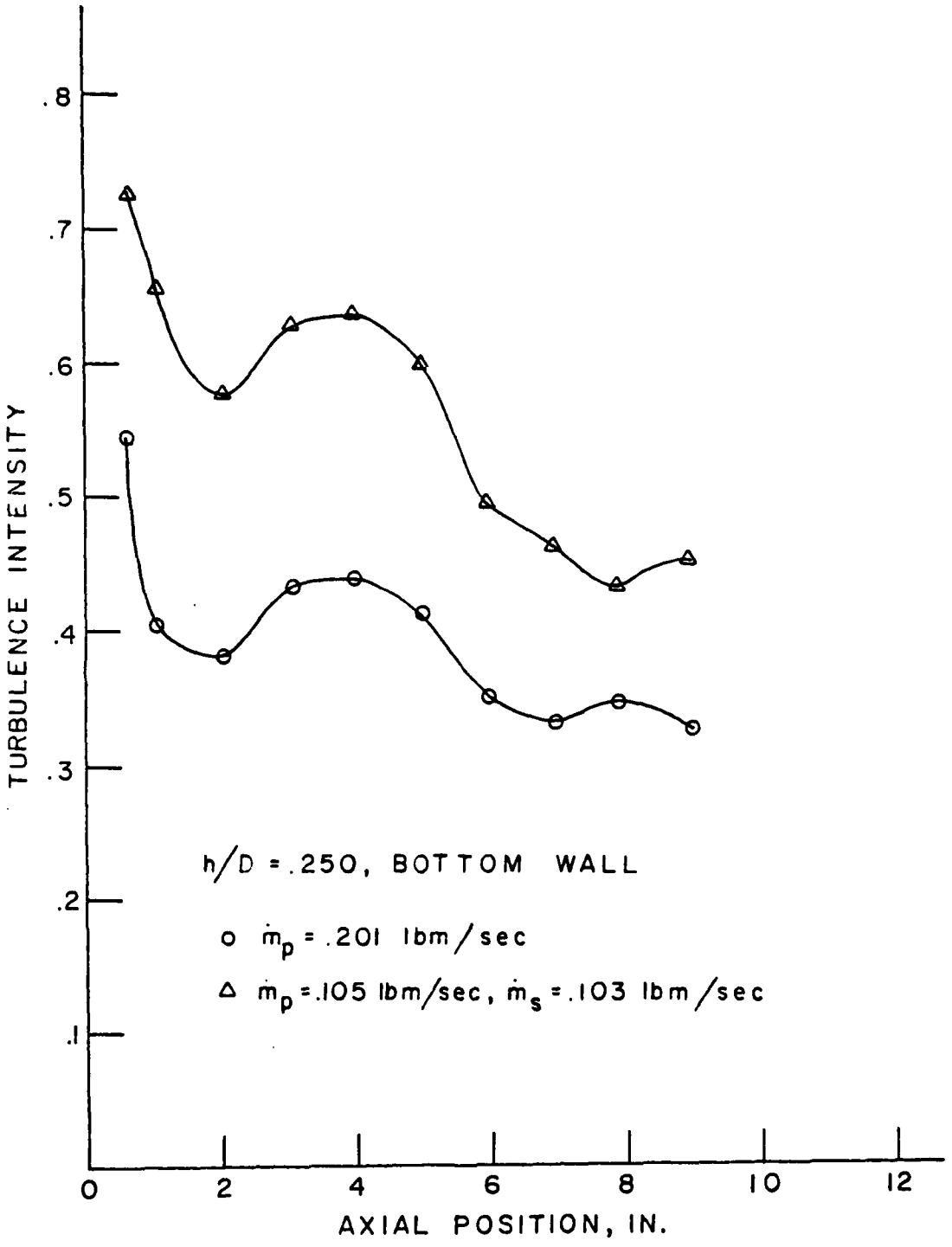

Fig. 27. Bottom Wall Turbulence Intensity, h/D = 0.250

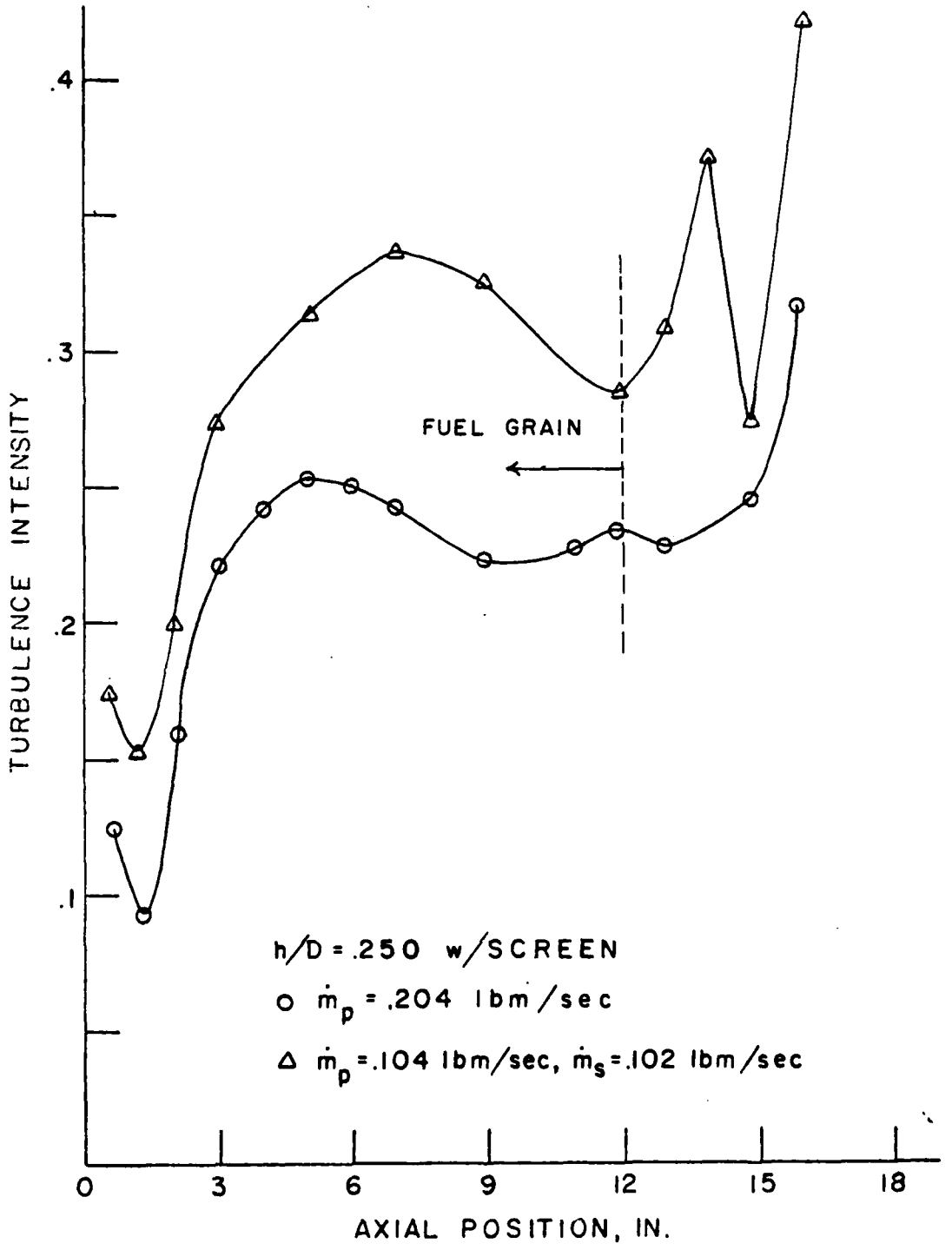

Fig. 28. Centerline Turbulence Intensity, Inlet Screen

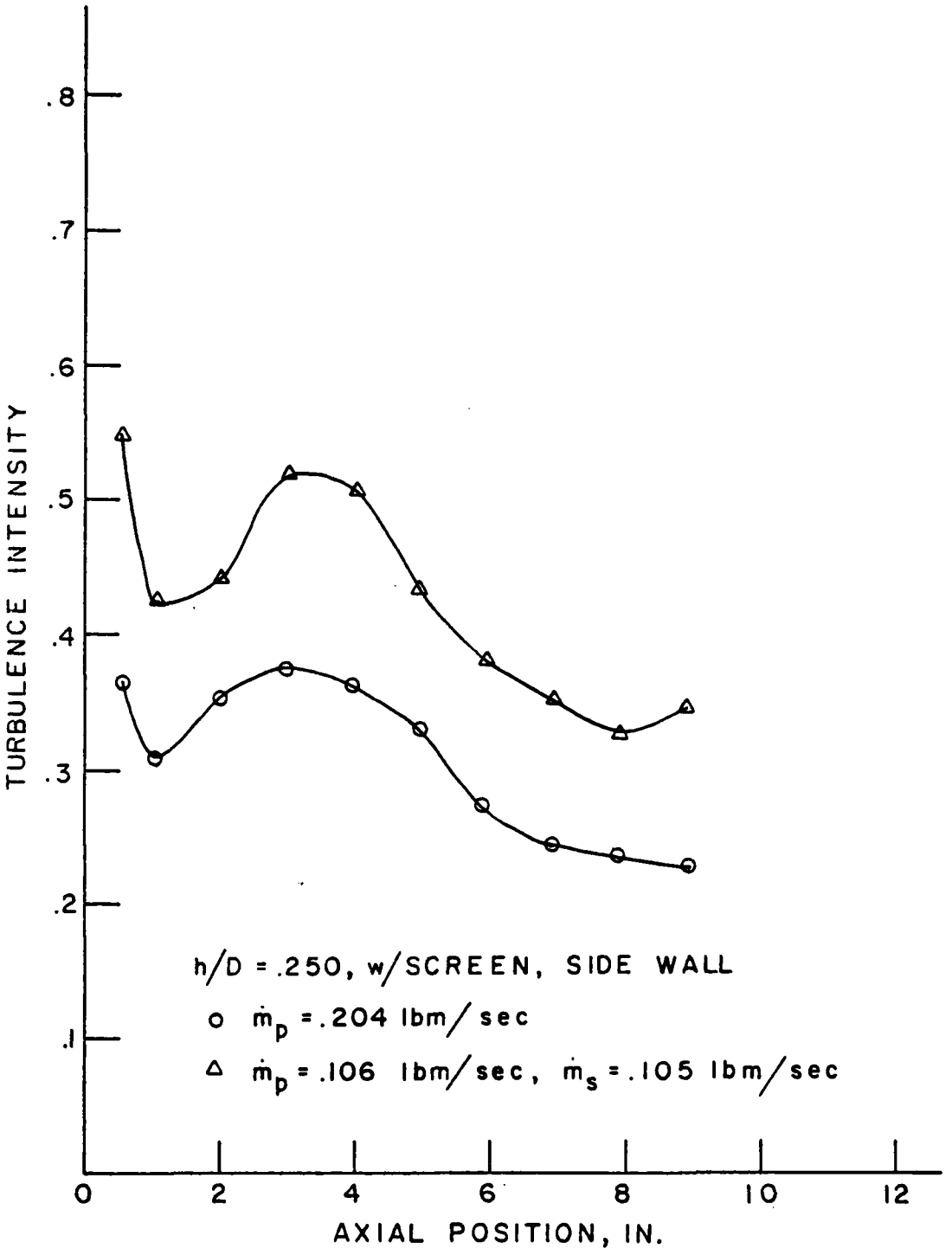

Fig. 29. Side Wall Turbulence Intensity, Inlet Screen

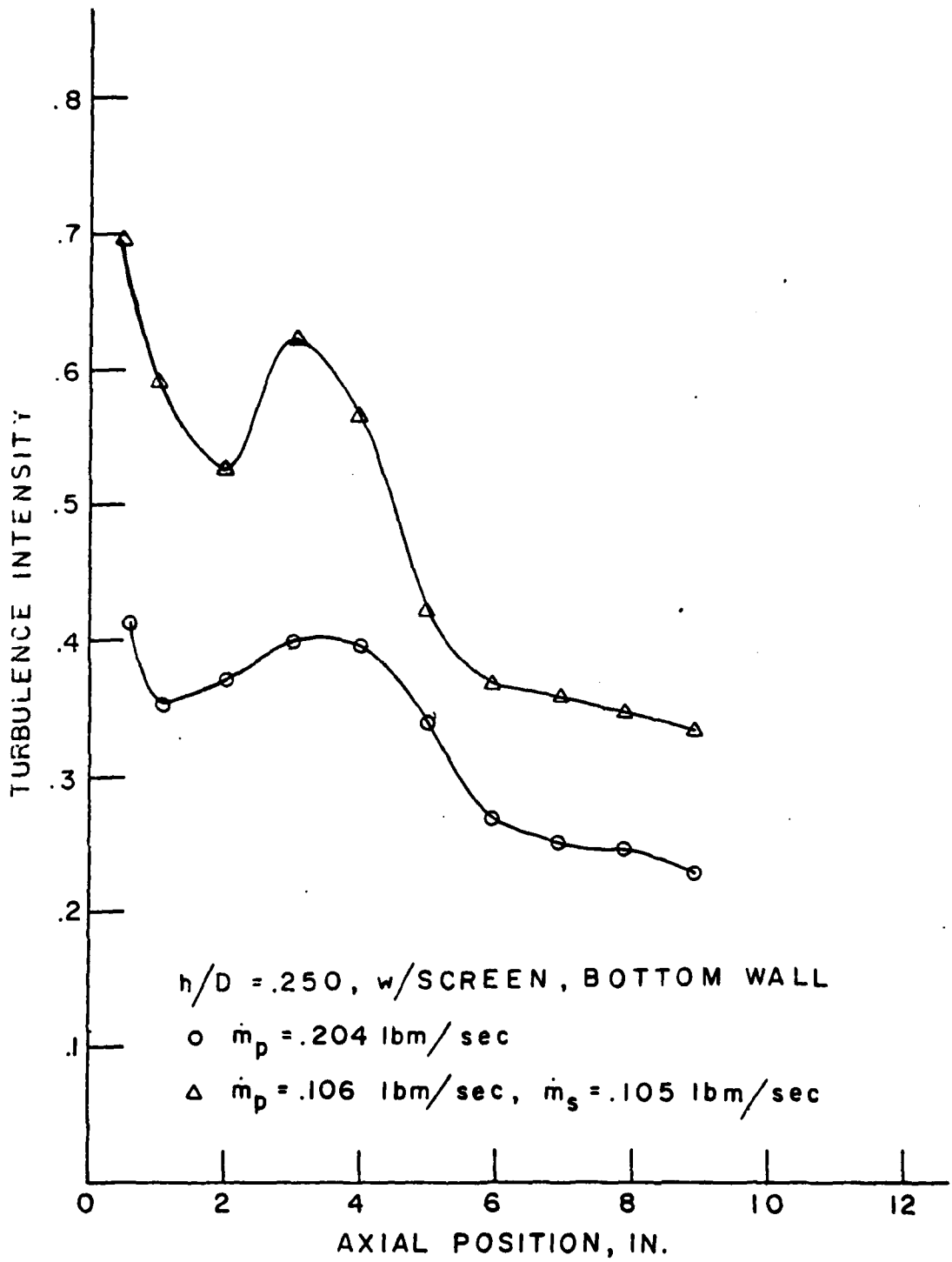

Fig. 30. Bottom Wall Turbulence Intensity, Inlet Screen

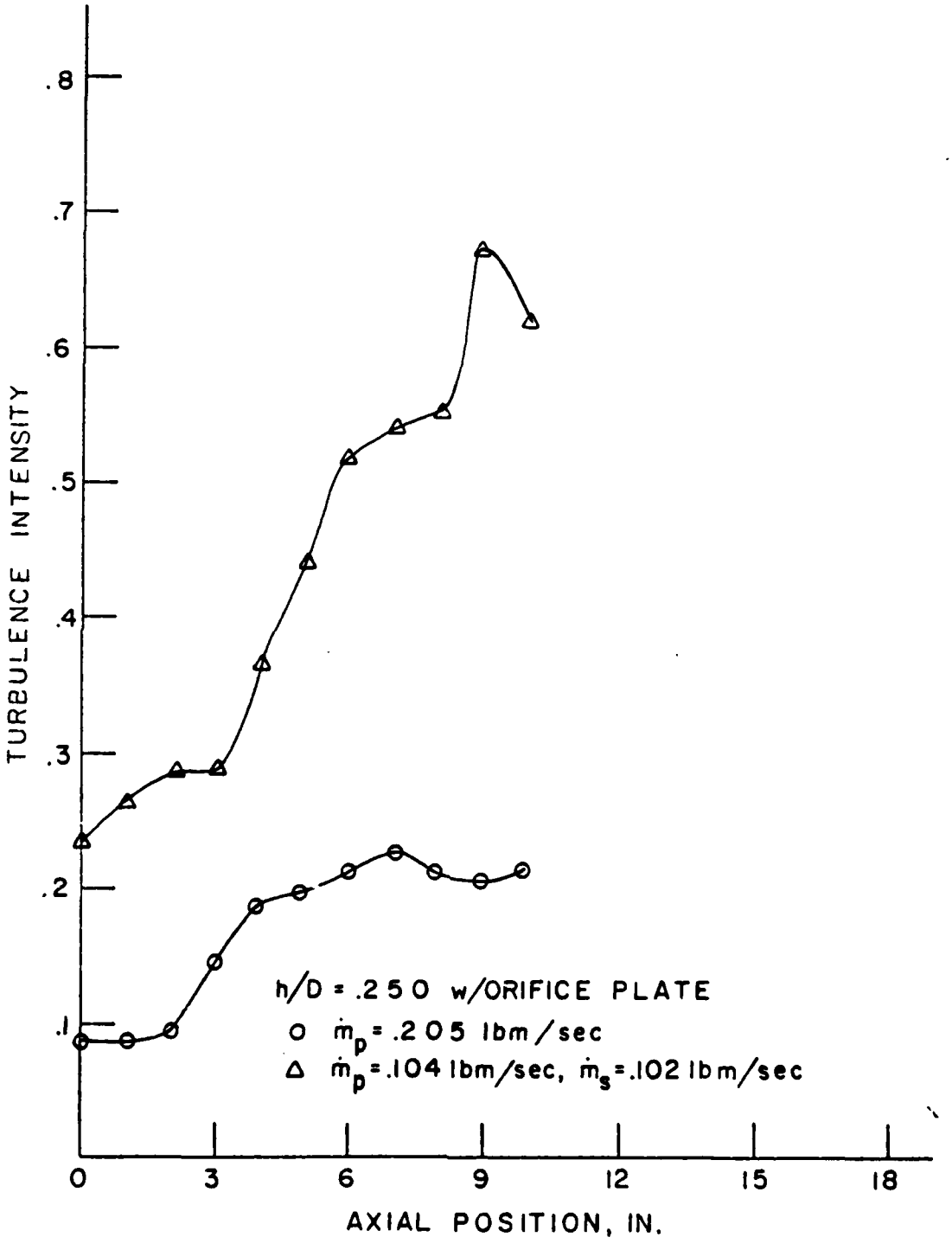

Fig. 31. Centerline Turbulence Intensity, Aft Orifice Plate

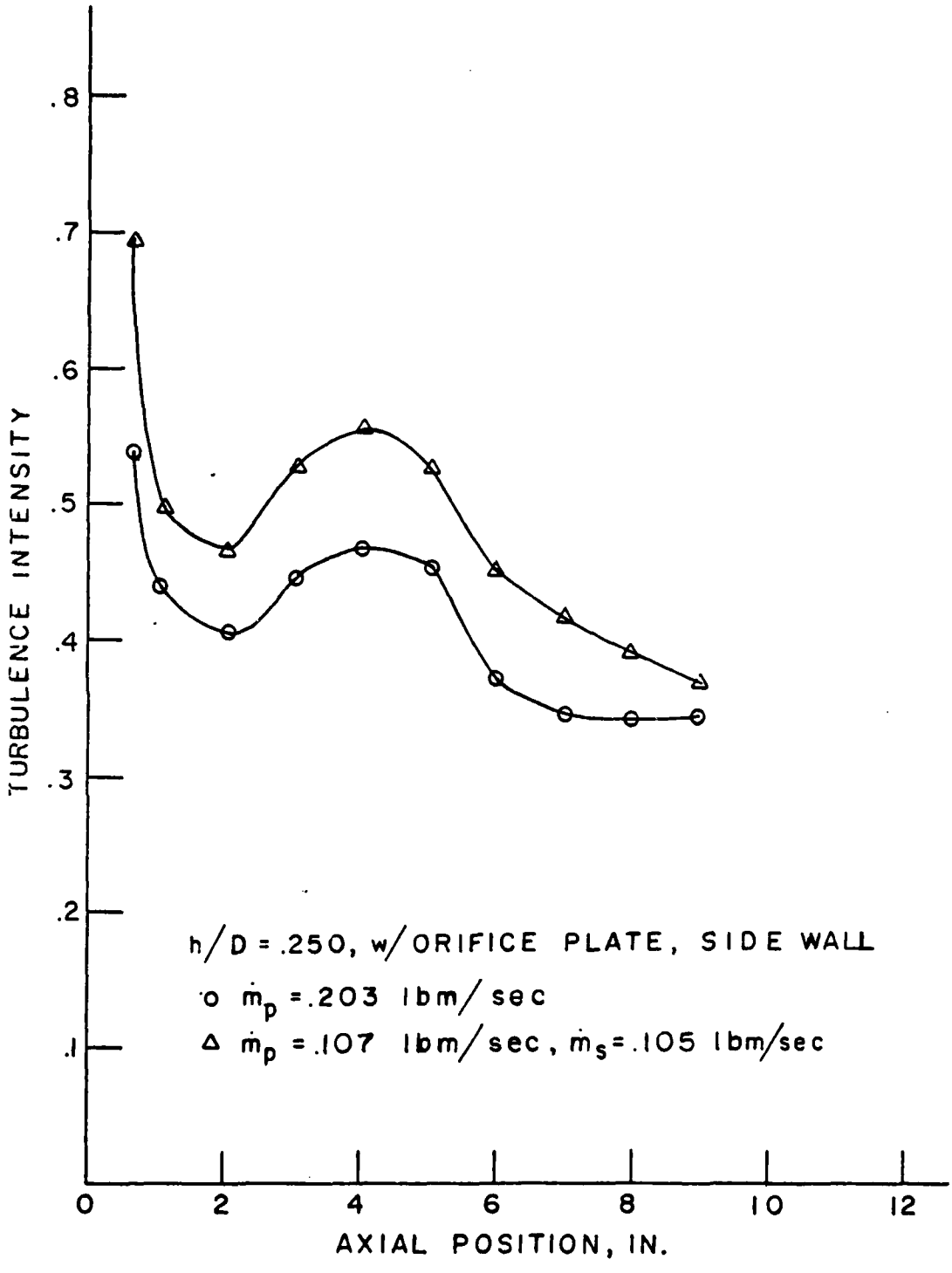

Fig. 32. Side Wall Turbulence Intensity, Aft Orifice Plate

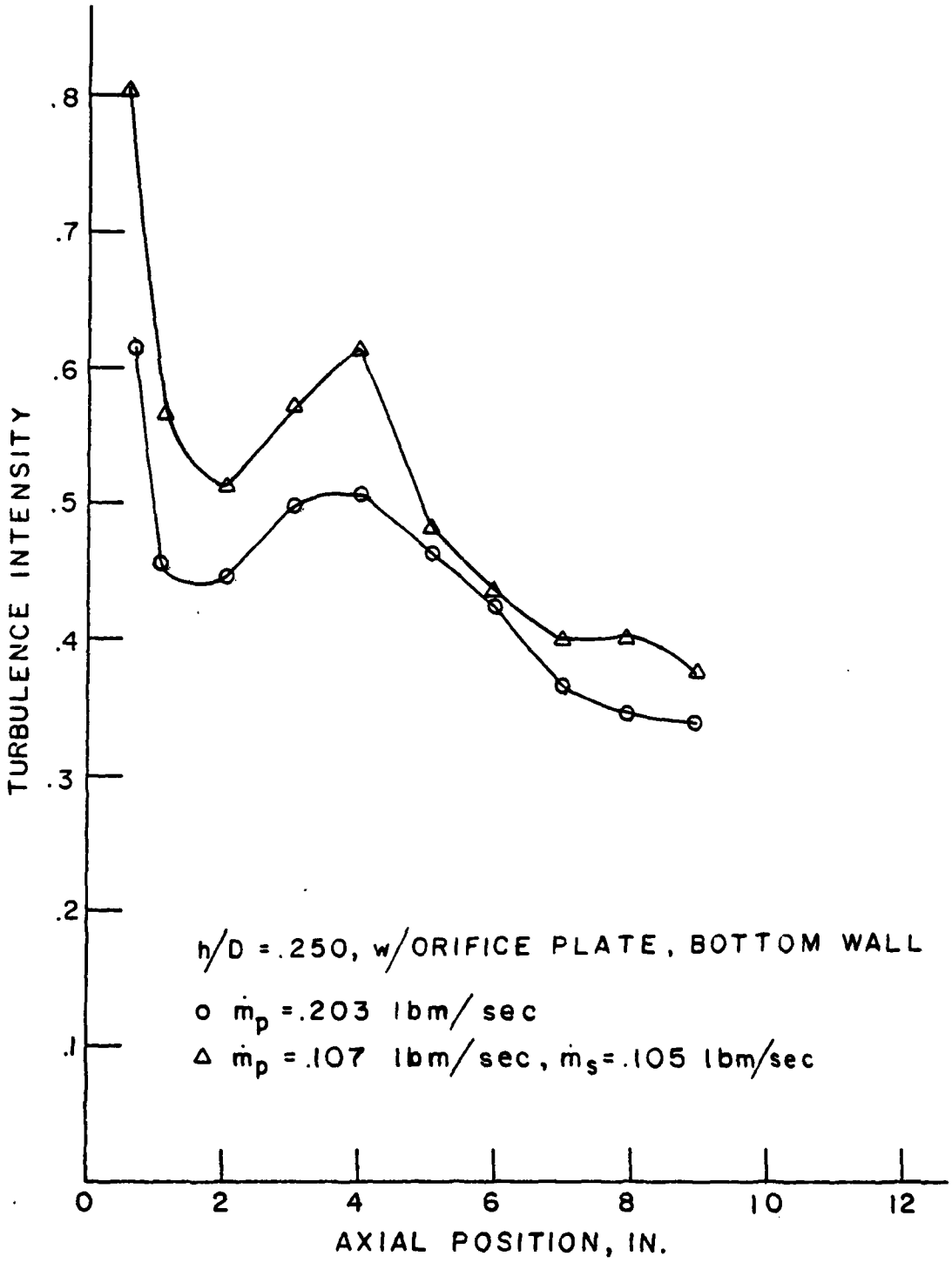

Fig. 33. Bottom Wall Turbulence Intensity, Aft Orifice Plate

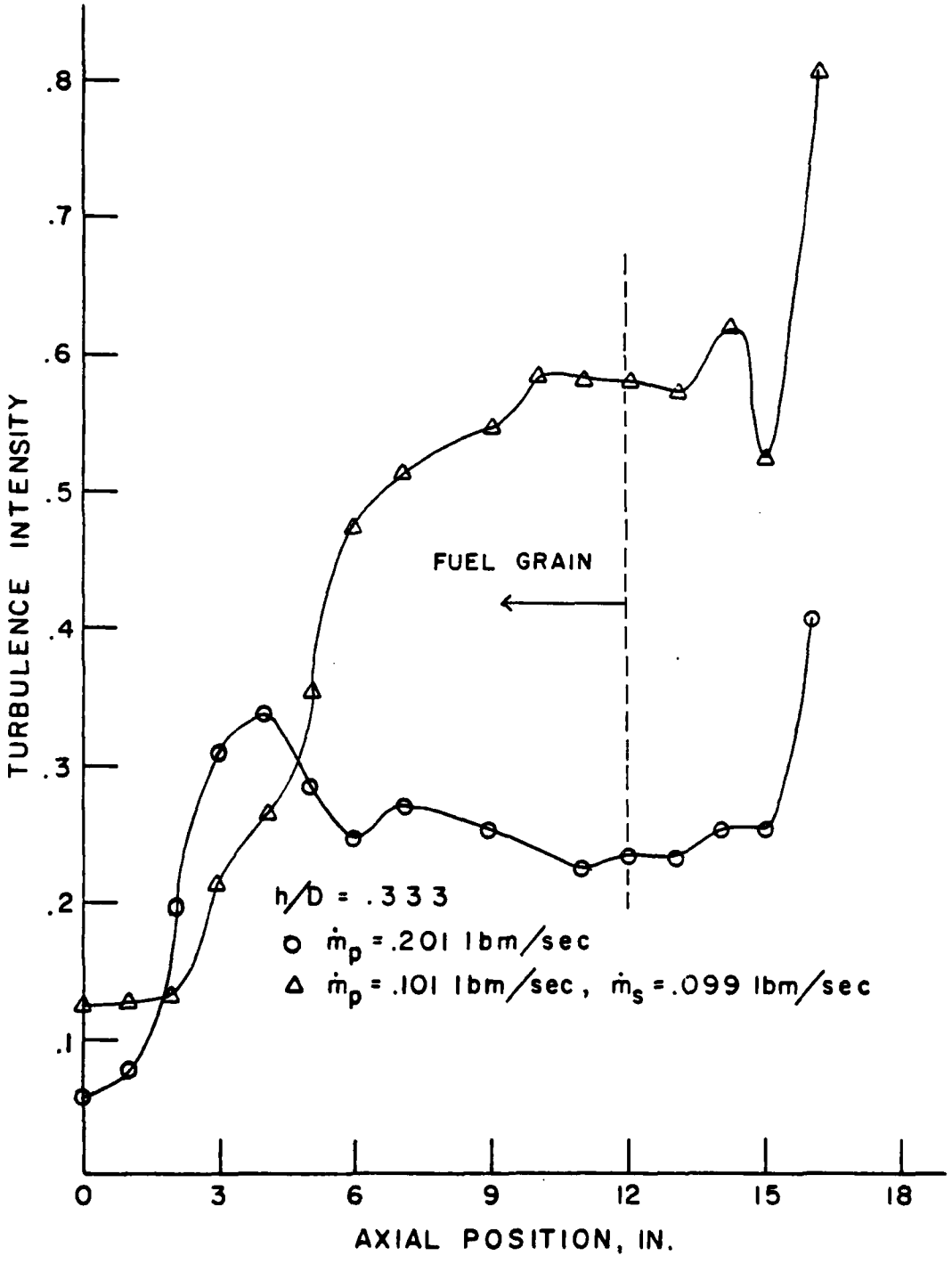

Fig. 34. Centerline Turbulence Intensity, h/D = 0.333

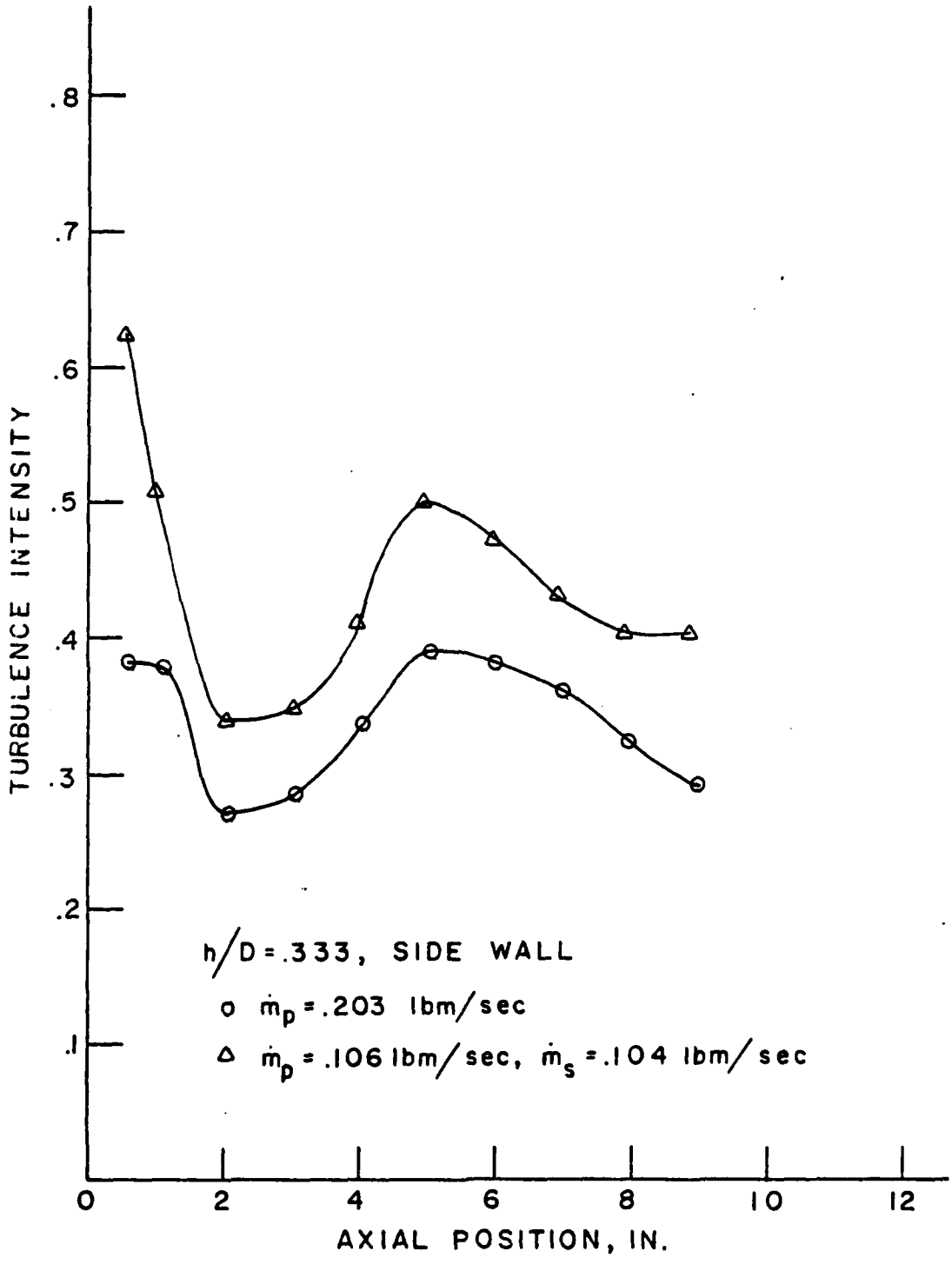

Fig. 35. Side Wall Turbulence Intensity, h/D = 0.333

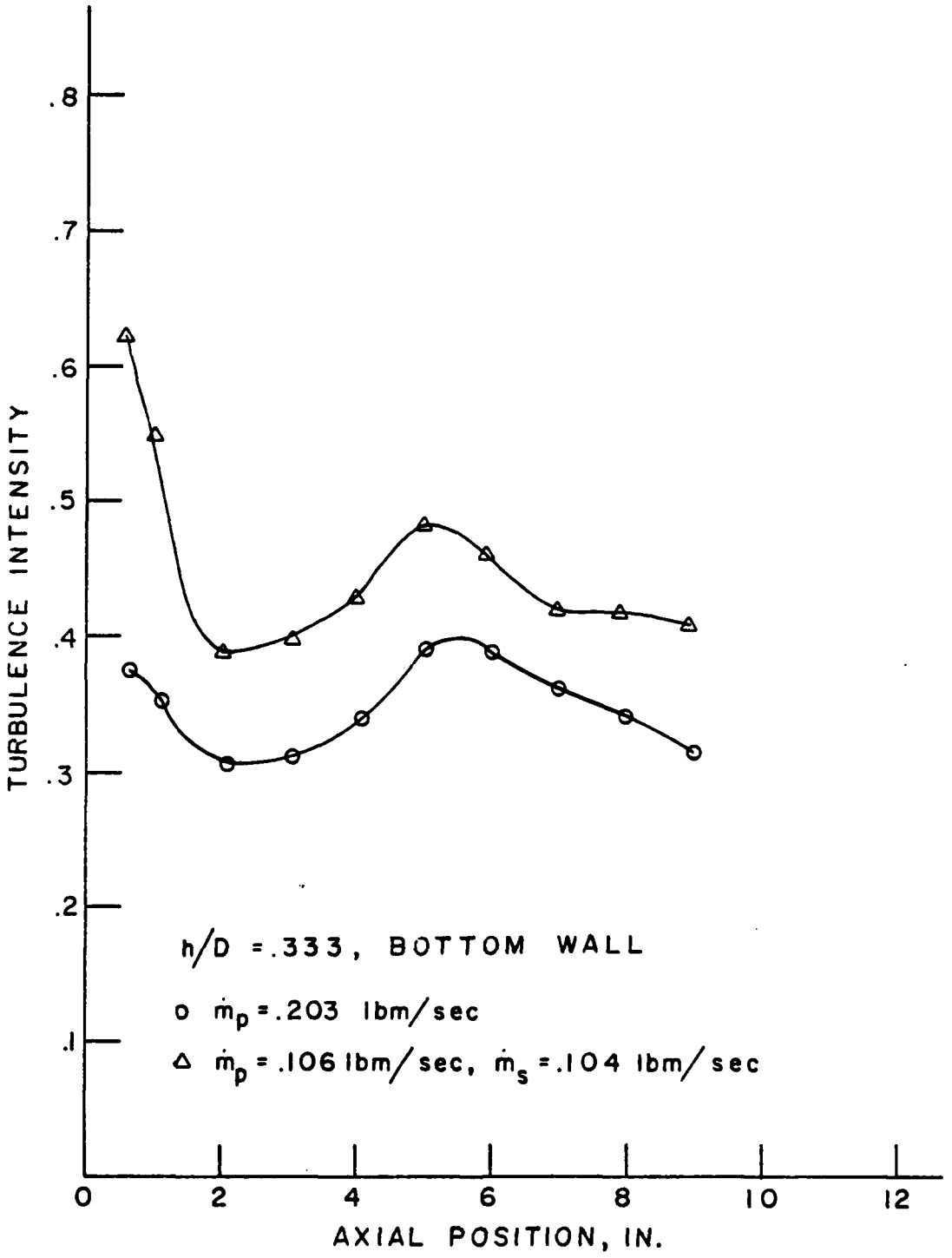

Fig. 36. Bottom Wall Turbulence Intensity, h/D = 0.333

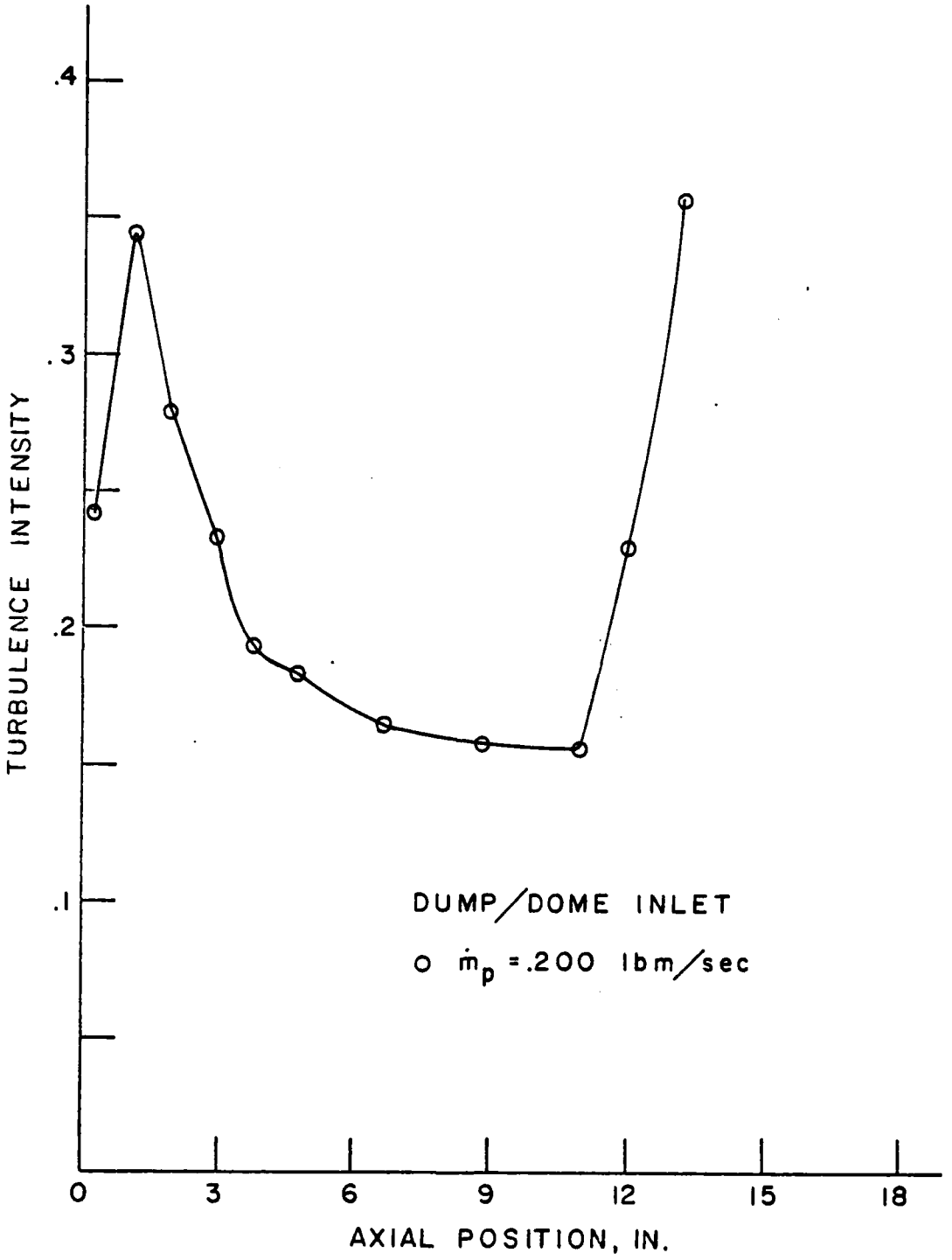

Fig. 37. Centerline Turbulence Intensity, Dump/Dome Inlet

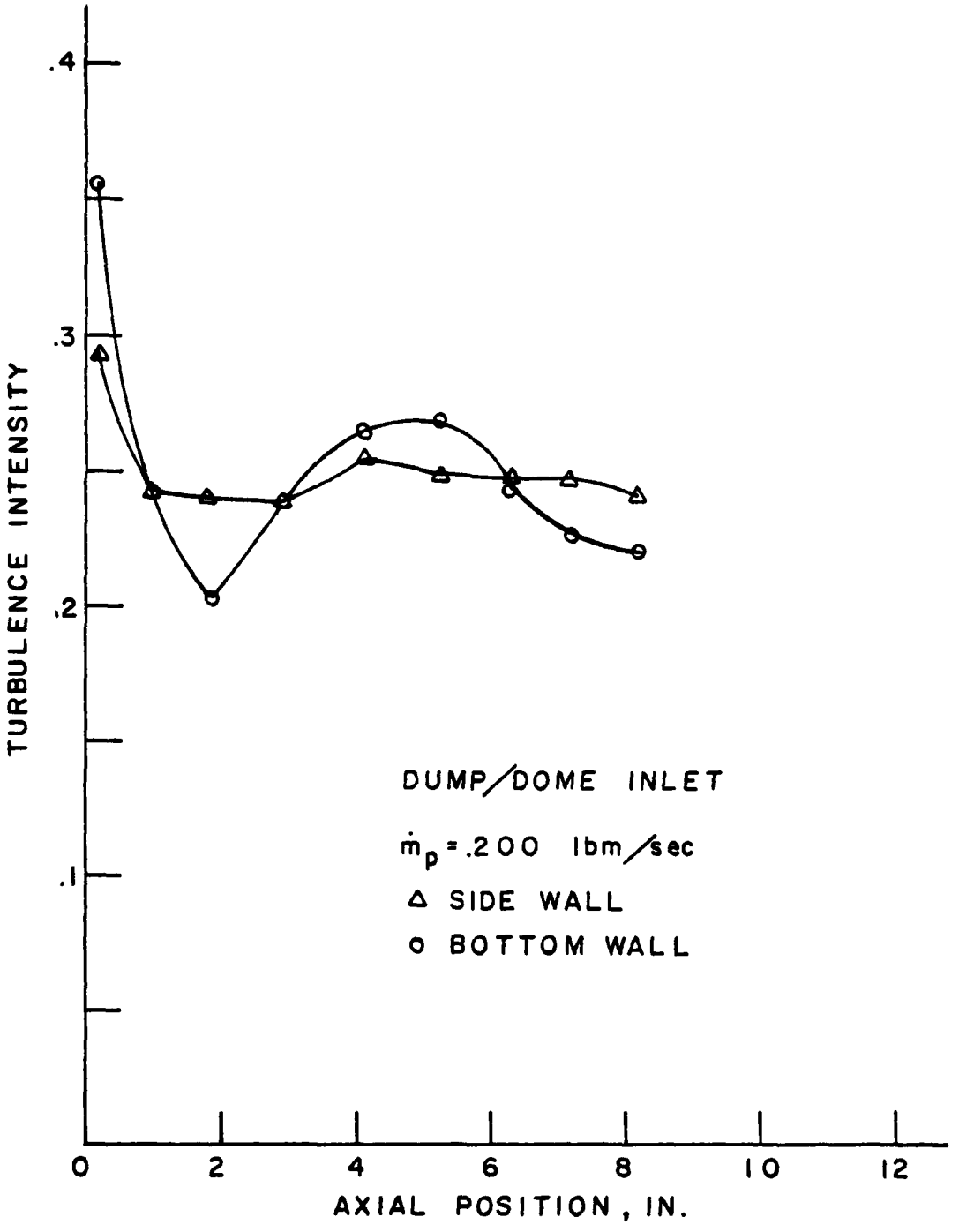

Fig. 38. Side/Bottom Wall Turbulence Intensity, Dump/Dome Inlet

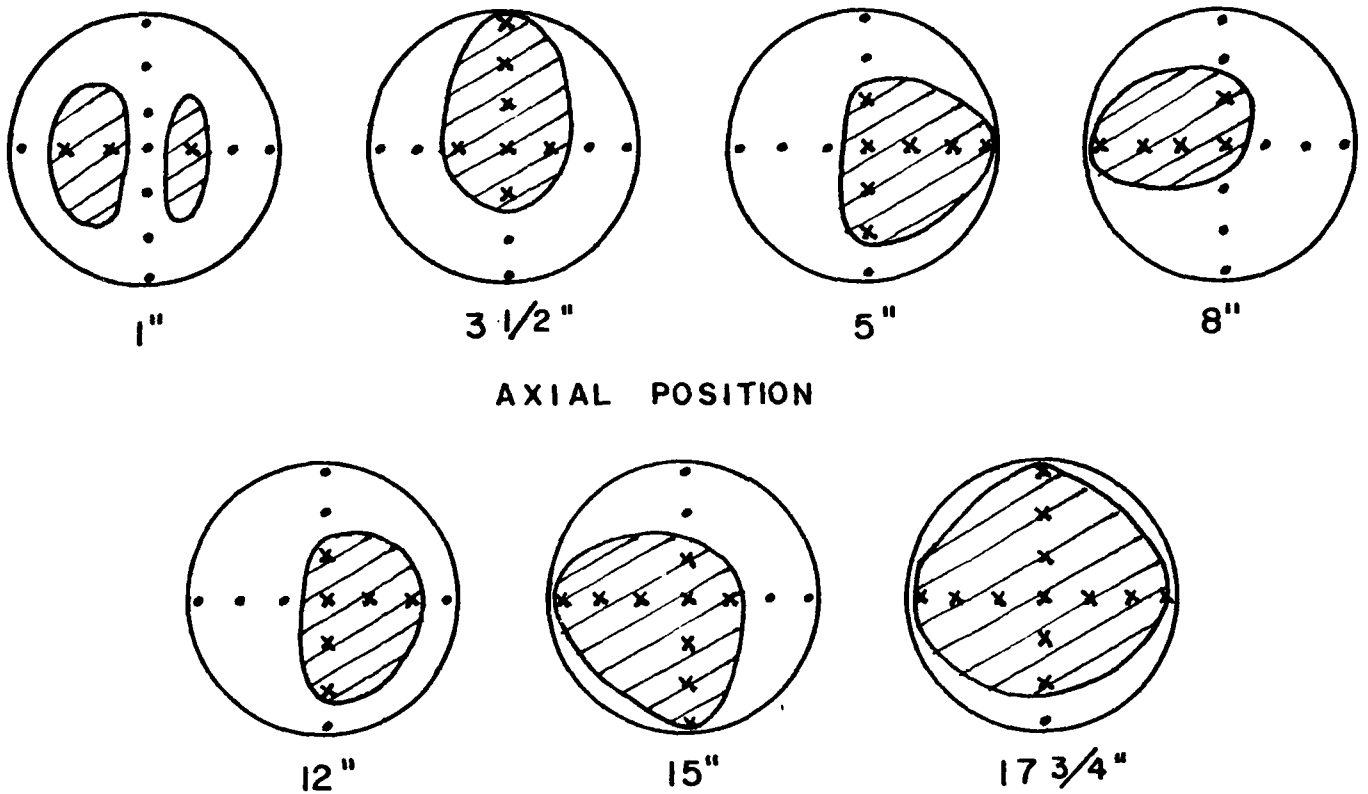

Fig. 39. Flow Regions in Ramjet Motor, Dump/Dome Inlet

INITIAL DISTRIBUTION LIST

		No. Copies
1.	Defense Technical Information Center Cameron Station Alexandria, VA 22314	2
2.	Library, Code 0142 Naval Postgraduate School Monterey, CA 93940	2
3.	Department Chairman, Code 67 Department of Aeronautics Naval Postgraduate School Monterey, CA 93940	1
4.	Professor D. W. Netzer, Code 67Nt Department of Aeronautics Naval Postgraduate School Monterey, CA 93940	2
5.	CAPTAIN Brian A. Binn, USAF 4814 Harvest Ct. Colorado Springs, CO 80917	2
6.	AFIT/CIR Wright-Patterson AFB, OH 45433	1